



Molecular changes associated with chronic liver damage and neoplastic lesions in a murine model of hereditary tyrosinemia type 1



Francesca Angileri^a, Vincent Roy^a, Geneviève Morrow^a, Jean Yves Scoazec^b, Nicolas Gadot^b, Diana Orejuela^{a,1}, Robert M. Tanguay^{a,*}

^a Laboratoire de génétique cellulaire et développementale, IBIS et PROTEO, Département de Biologie Moléculaire, Biochimie Médicale et Pathologie, Faculté de Médecine, 1030 Ave de la médecine, Université Laval, Québec G1V 0A6, Canada

^b Service Central d'anatomie et de Cytologie Pathologiques, Hôpital Edouard-Herriot, 69437 Lyon Cedex 03, France

ARTICLE INFO

Article history:

Received 15 March 2015

Received in revised form 28 August 2015

Accepted 4 September 2015

Available online 7 September 2015

Keywords:

ER stress

Hereditary tyrosinemia type 1 (HT1)

Metabolic diseases

Hepatoma

Liver dysfunction

HO-1

ABSTRACT

Hereditary tyrosinemia type 1 (HT1) is the most severe inherited metabolic disease of the tyrosine catabolic pathway, with a progressive hepatic and renal injury and a fatal outcome if untreated. Toxic metabolites accumulating in HT1 have been shown to elicit endoplasmic reticulum (ER) stress response, and to induce chromosomal instability, cell cycle arrest and apoptosis perturbation. Although many studies have concentrated on elucidating these events, the molecular pathways responsible for development of hepatocellular carcinoma (HCC) still remain unclear. In this study the *fah* knockout murine model (*fah*^{−/−}) was used to investigate the cellular signaling implicated in the pathogenesis of HT1. *Fah*^{−/−} mice were subjected to drug therapy discontinuation (Nitisinone withdrawal), and livers were analyzed at different stages of the disease. Monitoring of mice revealed an increasing degeneration of the overall physiological conditions following drug withdrawal. Histological analysis unveiled diffuse hepatocellular damage, steatosis, oval-like cells proliferation and development of liver cell adenomas. Immunoblotting results revealed a progressive and chronic activation of stress pathways related to cell survival and proliferation, including several stress regulators such as Nrf2, eIF2α, CHOP, HO-1, and some members of the MAPK signaling cascade. Impairment of stress defensive mechanisms was also shown by microarray analysis in *fah*^{−/−} mice following prolonged therapy interruption. These results suggest that a sustained activation of stress pathways in the chronic HT1 progression might play a central role in exacerbating liver degeneration.

© 2015 Elsevier B.V. All rights reserved.

1. Introduction

Hereditary tyrosinemia type 1 (HT1, OMIM 276700) is a severe autosomal recessive disorder characterized by impairment of fumarylacetoacetate hydrolase (FAH), the last enzyme in tyrosine degradation pathway (Fig. 1). FAH is mainly expressed in liver and kidneys, and loss of its activity results in accumulation of toxic metabolites such as fumarylacetoacetate (FAA) and succinylacetone (SA), leading to a progressive deterioration of renal and hepatic functions [1–8]. HT1 arises early in childhood and presents three different clinical forms: acute, subacute and chronic [9]. The acute form is characterized by lethal hepatic failure associated with cirrhosis, hepato- and splenomegaly, leading to death in the first months of life. The subacute form

(second half of the first year) manifests a similar but less severe clinical picture presenting usually with failure to thrive, hepatomegaly, easy bruising and hypophosphatemic rickets (due to a tubular dysfunction). In the chronic form (after the first year) patients show renal and hepatic dysfunction, vitamin-D resistant rickets, growth retardation, neurological crisis and hepatocellular carcinoma (HCC). The toxic actions of FAA are thought to be responsible for renal and hepatic failure as well as for the development of HCC [5,10–12]. Indeed several studies have reported FAA as a mutagenic and apoptogenic compound [5,10,11], and as cause of oxidative damage by forming stable adduct with glutathione (GSH) and sulphhydryl groups of proteins [13,14]. In addition, FAA induces tumor hypoxia [15] and genomic instability [5,16]. Still further contribution to the establishment of the sustained stress environment is the alkylating capacity of FAA and maleylacetoacetate (MAA) reduction products, fumarylacetone (FA) and maleylactone (MA) [17]. Accumulation of toxic products in liver and kidney cells can be prevented by treating HT1 patients with NTBC (2-[2-nitro-4-(trifluoromethyl)benzoyl]cyclohexane-1,3-dione, or Nitisinone), an inhibitor of p-hydroxyphenylpyruvate dioxygenase (HPPD), an enzyme upstream of FAA production (Fig. 1). Currently, NTBC therapy, in

* Corresponding author at: Laboratoire de Génétique Cellulaire et Développementale, Institut de Biologie Intégrative et des Systèmes (IBIS) et PROTEO, Dép. de Biologie Moléculaire, Biochimie Médicale et Pathologie, Pavillon CE-Marchand, 1030 Avenue de la Médecine, Université Laval, Québec G1V 0A6, Canada.

E-mail address: Robert.tanguay@fmed.ulaval.ca (R.M. Tanguay).

¹ Present address: EFORT, Zurich, Switzerland.

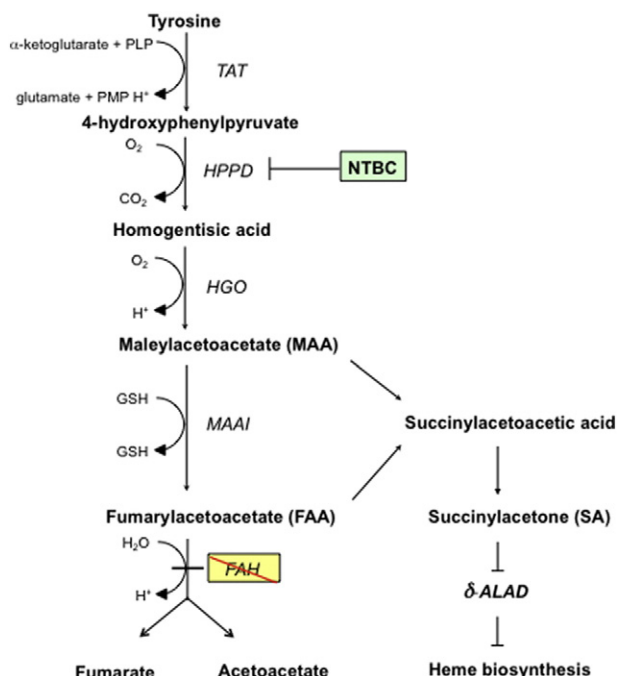


Fig. 1. The five enzymatic reactions of the tyrosine catabolic pathway. The GSH non-enzymatic bypass for transformation of MAA into FAA is also indicated. δ -ALAD is inhibited by succinylacetone causing δ -ALA accumulation and inhibition of heme biosynthesis. TAT, tyrosine aminotransferase; PLP, pyridoxal phosphate; PMP, pyridoxamine phosphate; HPPD, 4-hydroxyphenylpyruvate dioxygenase; HGO, homogentisate dioxygenase; MAAI, maleylacetoacetate isomerase; FAH, fumarylacetoacetate hydrolase; NTBC, 2-(2-nitro-4-(trifluoromethyl)benzoyl)cyclohexane-1,3-dione; δ -ALAD, δ -aminolevulinic acid dehydratase. Marked FAH indicates loss of function of this enzyme in HT1 patients.

combination with a diet low in tyrosine, and orthotopic liver transplantations for more severe cases, are the only treatments available for HT1 patients [18,19]. Although the efficacy of this drug improves greatly the lifestyle of patients, late complications can persist. Moreover recent data described the occurrence of HCC in some HT1 subjects, even under NTBC therapy [19–22]. In this regard, many efforts have been made in understanding the origin of damages occurring in HT1, but the cellular mechanisms underlying the progression of this pathological condition are not fully understood. When FAH-deficient mice are treated with NTBC, they avoid early lethality; however, a high percentage of NTBC-treated mice develop hepatocellular dysplasia after 7 months and 13–20% develop liver cancer after 18–24 months even when using a regimented therapy (i.e. a higher NTBC dose of 4 mg/kg/day plus dietary tyrosine restriction) [23,24]. Arising evidences from this murine model suggest an important metabolic impairment in FAH-deficient livers due to toxicity of the tyrosine-derived compounds.

In the present study, the *fah* knockout mouse model (*fah*^{−/−} mouse) was used in order to investigate the molecular pathways involved in the development and progression of HT1 pathogenesis. By a slight protocol modification, we were able to extend the survival of *fah*^{−/−} mouse in absence of NTBC treatment from 5 to 15 weeks, therefore enabling the study of HT1 progression on a longer period than previous studies and most importantly until the appearance of neoplastic damages. Here we report a stepwise activation of stress response pathways induced by FAH impairment. The first changes were observed within the first week of NTBC withdrawal as soon as the inhibitory action of the drug becomes less effective, while the second phase appeared 4 weeks after NTBC interruption and was accompanied by AFP up-regulation. Protein expression patterns revealed an important crosslink among survival mechanisms in chronic liver dysfunction. To corroborate these results, we performed microarray profiling in mouse livers subjected to long-term NTBC withdrawal. Analysis of microarray data showed an altered expression of gene transcripts associated with differentiated hepatic

functions and cell proliferation that occurred as a result of the chronic damage induced by HT1 stress. The most affected pathways include those involved in oxidative stress and detoxification, inflammation-cytokine-chemokine systems, hepatic fibrosis and cellular growth. Moreover, different transcripts associated with cancer progression were found to be highly up-regulated in this stage.

2. Material and methods

2.1. Animals

Four months-old *fah* knockout (*fah*^{Δ_{exon5}}, referred to here as *fah*^{−/−}) male mice were used as model for human HT1 [25]. All animals were fed with a standard rodent chow (Charles River Rodent, Purina 5075-U.S, Agribrands St.Hubert, QC, Canada) containing 0.51% tyrosine and 0.82% phenylalanine, and housed in a controlled environment with 12 h light–dark cycles. Pregnant females and pups *fah*^{−/−} were treated with 2-(2-nitro-4-(trifluoromethyl)benzoyl)cyclohexane-1,3-dione (NTBC) in drinking water (7.5 mg/L, pH 7–7.3) until beginning of experimentation. NTBC was generously provided by S. Lindstedt (Gothenburg University, Sweden).

2.2. Treatment

To induce the HT1 phenotype, 4 months-old *fah*^{−/−} mice were withdrawn from NTBC therapy for periods of three days to 15 weeks. Mice were weighted three times per week and periodically examined for signs of clinical illness. At the end of each starvation period, three to ten mice were euthanized by an overdose of ketamine-xylazine cocktail (2–3 times the anesthetic dose) followed by cervical dislocation. *Fah*^{−/−} mice receiving NTBC *ad libitum* (n = 5) were used as healthy control. Fragments of harvested livers were processed for histology and the remaining tissues were snap-frozen in liquid nitrogen and stored at −80 °C until analysis. All procedures for animal use were approved by the local animal care comity (CPA-UL) according to the Canadian Council on Animal Care (CCAC) recommendations.

2.3. Histological analysis

Mouse livers were dissected, examined for gross features, fixed in 4% PBS-buffered paraformaldehyde, pH 7.4, and kept at 4 °C. Tissue samples were embedded in paraffin-wax at 58 °C. Four micrometer sections were prepared and stained with hematoxylin-eosin-saffron (HES), Sirius Red for demonstration of fibrosis and reticulin stain for analysis of liver architecture. Immunohistochemistry was performed on deparaffinized tissue sections with an anti-cleaved caspase-3 antibody (rabbit polyclonal antibody, Cell Signaling, Danvers, MA) for demonstration of apoptosis and with an anti-glutamine synthetase antibody (mouse monoclonal antibody clone 6, BD Biosciences, San Jose, CA) for analysis of liver zonation; an indirect immunoperoxidase technique performed according to the streptavidin-biotin method was used. All techniques were performed at ANIpath, a university platform for experimental animal histopathology (Lyon, France). Analysis and interpretation were done by a pathologist experienced in both human and experimental liver pathologies (JYS). Diagnosis and classification of liver changes were performed according to international recommendations [26].

2.4. Immunoblotting

For Western blot analysis frozen livers were homogenized with a teflon-glass pestle at 10% (W/V) in RIPA Buffer (20 mM Tris–HCl, pH 7.5; 150 mM NaCl; 1 mM Na₂EDTA; 1 mM EGTA; 1% NP-40) with protease inhibitor cocktail tablets (cOmplete, Mini, EDTA-free; Roche Diagnostics, Indianapolis, USA) and phosphatase inhibitor cocktail tablets (PhosSTOP; Roche Diagnostics, Indianapolis, USA). The homogenized

extracts were centrifuged at 10,000 g for 15 min at 4 °C. Protein concentration was measured with the Bio-Rad Protein Assay (Bio-Rad Laboratories Inc., Hercules, CA). Proteins were resolved by electrophoresis on a 12% SDS-PAGE gel, transferred onto a nitrocellulose blotting membrane (BioTrace NT, Pall Life Sciences), blocked with 5% non-fat dried milk in TBS (Tris-buffered saline; 50 mM Tris, 150 mM NaCl, pH 7.5) and incubated overnight at 4 °C with primary antibodies following recommendations by the manufacturers. Antibodies against Nrf2 (1:1000; #12,721), CHOP (1:1000; #2895), Bcl2 (1:1000; #2870), phospho-Bad (Ser112) (1:2000; #9296), phospho-Bad (Ser136) (1:1000; #5286), Mcl-1 (1:1000; #5453), Erk1/2 (1:1000; #4695), phospho-ERK1/2 (Thr202/Tyr204) (1:1000; #4370), MEK1/2 (1:1000; #9122), phospho-MEK1/2 (Ser217/221) (1:1000; #9121), phospho-PKC (pan, γ Thr514) (1:1000; #9379) were from Cell Signaling Technology (Danvers, MA, USA). Antibody against AFP (1:10,000) was a gift from Dr. L. Bélanger (CRCHUQ, QC, Canada). HO-1 antibody (1:10,000; #ab13248) was from Abcam (Toronto, ON, Canada). Phospho-eIF2 α (Ser51) (1:1000; #KAP-CP130) was purchased from Stressgen (Victoria, BC, Canada). Antibodies for BAX (1:1000; #RB-063-P0) (NeoMarkers, Fremont, CA, USA) and PKC (pan) (1:1000; #SAB4502356) (Sigma-Aldrich Canada Co., Oakville, ON, Canada) were also used. Goat anti-mouse IgG or goat anti-rabbit IgG peroxidase-conjugated (1:5000; #115-035-146 and #111-035-144 respectively) (Jackson ImmunoResearch Lab, West Grove, PA, USA) were used as secondary antibodies. Since commonly used reference proteins (e.g. β -actin; α - β - γ -tubulin) were differently modulated in HT1 mice, we selected the stably expressed HSP60 as loading control (1:10,000; #37) [27]. Signals were revealed with Clarity™ Western ECL Substrate (Bio-Rad, Hercules, CA, USA) using the Odyssey® Infrared Imaging System (Li-COR, Biosciences, Lincoln, NE, USA). Densitometric analysis on Western blot bands was performed using ImageJ 1.47v software. Values were normalized to loading control levels and finally compared to the *fah*^{-/-} healthy control (NTBC-treated). Data in histograms indicate the average of four mice for each time point, with error bars indicating standard deviation.

2.5. RNA isolation

Total RNA was obtained from snap-frozen liver tissues using mirVana™ PARIS™ Kit (Life Technologies, Burlington, ON, Canada) according to the manufacturer's instructions. Purified total RNA was eluted in RNase-Free water followed by DNase-I digestion using the RNase-free DNase kit and RNeasy spin column (QIAGEN, Mississauga, ON). The quality and purity of RNA samples were checked by capillary electrophoresis using the Agilent 2100 Bioanalyzer and Agilent RNA Nano 6000 LabChip kits (Agilent Technologies, Santa Clara, CA, USA).

2.6. Gene expression analysis

To analyze gene expression profile of *fah*^{-/-} mice during chronic liver injury, equivalent amounts of total RNA from four mice discontinued from therapy for 7–8 weeks was pooled and amplified using the two colors Agilent Low Input Quick Amp Labeling kit protocol. A pool of *fah*^{-/-} healthy control mice ($n = 3$) was used as normalization control. Starting with 200 ng of total RNA, cyanine (Cy)3- or Cy5-labeled cRNA was produced according to the manufacturer's protocol. For each two-color comparison, 750 ng each of Cy3- and Cy5-labeled cRNA was mixed and fragmented using the Agilent In Situ Hybridization Kit protocol (Agilent Technologies, Santa Clara, CA, USA). Hybridizations were carried out with the Agilent Two-Color Microarray-based gene expression platform using the 4 × 44K Two Colors Mouse Whole Genome Microarray, 41,534 genes (Agilent Technologies, Santa Clara, CA, USA). Two hybridizations with fluorescent dye reversal technique (dye-swap) were performed for each RNA sample from each group. Slides were washed as indicated in Agilent's protocol and scanned using an Agilent DNA Microarray Scanner. The Cy3/Cy5 intensity data were extracted using Agilent's Feature Extraction software (Agilent

Technologies, Santa Clara, CA, USA). Values of genes in *fah*^{-/-} mice (NTBCw/o) were normalized against control samples (NTBC). Transcriptome analysis was performed using Agilent Genespring GX11 software (FRSQ-Réseau Cancer Core Genome Facility, Hôtel-Dieu, Québec, Canada).

2.7. Functional genomics analysis

The genes signature was further analyzed with Ingenuity Pathways Analysis (IPA Ingenuity software, QIAGEN, Redwood City, CA, USA). A fold change cutoff of 2-fold and $p < 0.001$ was set to identify genes whose expression was considered to be significantly regulated. Biologically relevant networks were drawn from the lists of genes differentially expressed in untreated (NTBCw/o) and treated *fah*^{-/-} mice. Core analysis was processed using direct and indirect relationships for pathway scoring (the complete list of deregulated genes is available upon request).

2.8. Statistical analysis

Comparisons between different experimental groups were made using one-way ANOVA with a Dunnett's post-hoc analyses (Prism). Results are means \pm standard deviation, p values ≤ 0.05 were considered statistically significant. Statistical significance is represented by asterisks.

3. Results

3.1. The *fah* knockout mouse model as an approach to understand liver dysfunction and hepatocarcinogenesis in HT1 patients

The *fah* ^{Δ exon5} mouse strain (*fah*^{-/-} mouse) [23,25] has already been extensively used as a useful model of human HT1 [7,28,29]. This model presents most of the phenotypic and biochemical manifestations of human HT1 on an accelerated time scale [6,7,23,25]. However none of the previous studies has investigated the effects of the long-term stress activation after complete NTBC withdrawal, due to the high mortality rate in the post therapy interruption. Indeed, the mean survival of *fah*^{-/-} mice following NTBC withdrawal is around 4 to 5 weeks, when they die from liver failure accompanied by severe weight loss [7,8,30,31]. We noticed that the high mortality rate observed was often associated with dehydration and intestinal problems (black stools and digestive tract filling). Thus we modified the traditional protocol integrating the mice diet from the fourth week post-withdrawal with a daily dose of water-soaked grinded rodent's food in an attempt to alleviate these complications (Fig. 2A). This simple change in food presentation resulted in an unexpected considerable increase of the mean survival time (Fig. 2B), from 5 to more than 15 weeks after NTBC discontinuation. The severe weight loss previously reported during the first 5 weeks following NTBC removal was followed by a stabilization of the mean weight and even an increase in weight up to 15 weeks (Fig. 2C). Each time point was chosen as representative of different stages of HT1 stress. In mice, NTBC has a biphasic kinetic of elimination with an initial phase having a half-life of 2.7 h and a subsequent phase having a half-life of 54 h [32], which corresponds to the mean terminal plasma half-life of NTBC in human (~54 h, DrugBank DB00348, <http://www.drugbank.ca/drugs/DB00348>). While a small amount of NTBC persists in the liver and kidneys up to seven days after a single dose, the complete inhibition of HPPD activity was observed only in the three first days after NTBC uptake [32] suggesting that FAA, MAA and SA starts to accumulate thereafter. We therefore chose three days of NTBC withdrawal as the first time point to start the evaluation of the early events induced by HT1 toxic metabolites accumulation. Livers of *fah*^{-/-} mice kept on NTBC from birth until time of sacrifice, were used as control.

Gross inspection of all *fah*^{-/-} mice under drug starvation revealed a progressive variation in liver/body weight ratio (L/BW) ($n = 3$ –10;

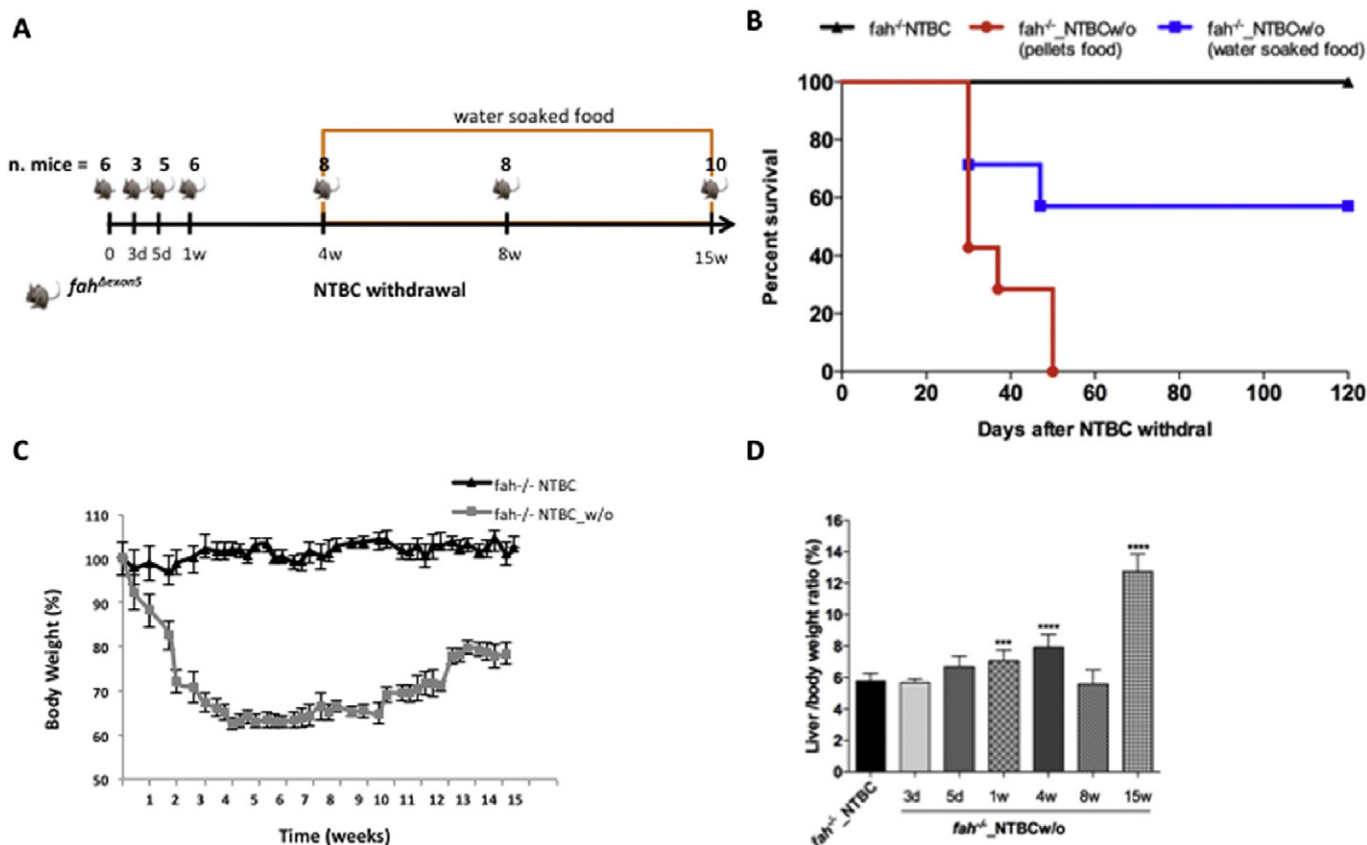


Fig. 2. Effect of NTBC withdrawal on mice weight and survival. (A) 15 weeks withdrawal protocol. Number of harvested mice per time point is indicated. Water soaked food treatment starts after 4 weeks of NTBC interruption. (B) Effect of water soaked food was evaluated on mice survival. Mice supplemented with water soaked food ($n = 7$) exhibited significantly increase in survival time against mice under regular diet ($n = 7$). (C) Body weight curves (%) for male $fah^{-/-}$ mice. Mice $fah^{-/-}$ NTBC-treated (\blacktriangle), and after NTBC-withdrawal (\blacksquare), were weighed three times per week. Each point in the curves represents the average of at least three mice, with error bars indicating standard deviation. (D) Liver/body weight ratio at different time point of $fah^{-/-}$ harvested mice. Results are means \pm s.d. ($n = 3$ –10) and are compared to the liver/body weight ratio of the control group (NTBC-treated); *** $p < 0.001$ and **** $p < 0.0001$.

Fig. 2D), with a considerable loss of abdominal fat (data not shown). Macroscopic appearance of livers in dissected mice was characterized by several dysmorphic changes, including the appearance of multiple nodules (Fig. 3). L/BW was up to 2.4-fold higher than normal after 15 weeks of drug starvation ($n = 10$; Figs. 2D and 3A,C). At the end point of 15 weeks of withdrawal, 100% of surviving mice ($n = 10$) revealed the presence of liver nodules. This long-range protocol permitted us to explore into more depth HT1-associated liver dysfunction and the process leading to neoplastic lesions that could eventually develop into HCC.

3.2. NTBC withdrawal induces acute liver failure with histologically evident hepatocellular changes

Histological examination showed that mild hepatocellular changes were present in $fah^{-/-}$ treated mice: hepatocytes were enlarged and presented very large, round nuclei containing several large nucleoli; many hepatocytes showed micro- and even macro-vesicular steatosis; there were no architectural changes and no fibrosis (Fig. 4A). The presence of such changes before therapy interruption suggests that NTBC treatment is not able to cover all damages induced by toxic metabolites accumulation, as previously reported [33,34]. Of note, MAA and FAA are highly reactive and considered as the primary causes of hepatocytes damage observed in HT1 [1,10,35,36]. After NTBC discontinuation, severe liver lesions, combining hepatocellular changes, inflammation and fibrosis were observed (Fig. 4B, C). Hepatocellular plates were disorganized, irregular and thickened. Hepatocytes were enlarged and

showed ballooning along with micro- and macro-vesicular steatosis; dysmorphic nuclei were present (Fig. 4B). Small inflammatory aggregates were scattered within liver lobules and proliferation of oval-like cells was observed mainly in the periportal areas of hepatic lobules. Oval-like cells were arranged in cohesive sheets or in pseudoglandular structures and were morphologically similar to the oval cells described at the initiation of the process of chemical carcinogenesis (Fig. 4B). Periportal and perisinusoidal fibrosis was present. Sirius Red staining of liver sections confirmed the presence of thin fibrotic septa extending from slightly enlarged portal tracts and running along preexistent sinusoids (Fig. 4C panel a). Finally, apoptotic figures were frequent and were highlighted by the immunohistochemical detection of cleaved caspase-3 (Fig. 4C panel b).

After 15 weeks of therapy interruption, the livers of $fah^{-/-}$ mice usually contained several nodules (Fig. 3C). Some nodules displayed features reminiscent of those presented by regenerative macro-nodules in human diseased liver: they contained fibrous septa running between normal hepatocyte plates. Other nodules were large and well demarcated (Fig. 5A). They showed the histological features of liver cell adenoma. They were formed by thickened hepatocellular plates, retaining a regular disposition (Fig. 5B) but devoid of the reticulin network associated with hepatocellular plates in the normal liver; only rare and dispersed reticulin fibers were present (Fig. 5C). No portal tract was visible. Large vessels were seen running through the tumor tissue. Tumor cells were monomorphic and characterized by increased nucleo-cytoplasmic ratio and basophilic cytoplasm; there was no significant cell atypia and only rare mitoses were observed

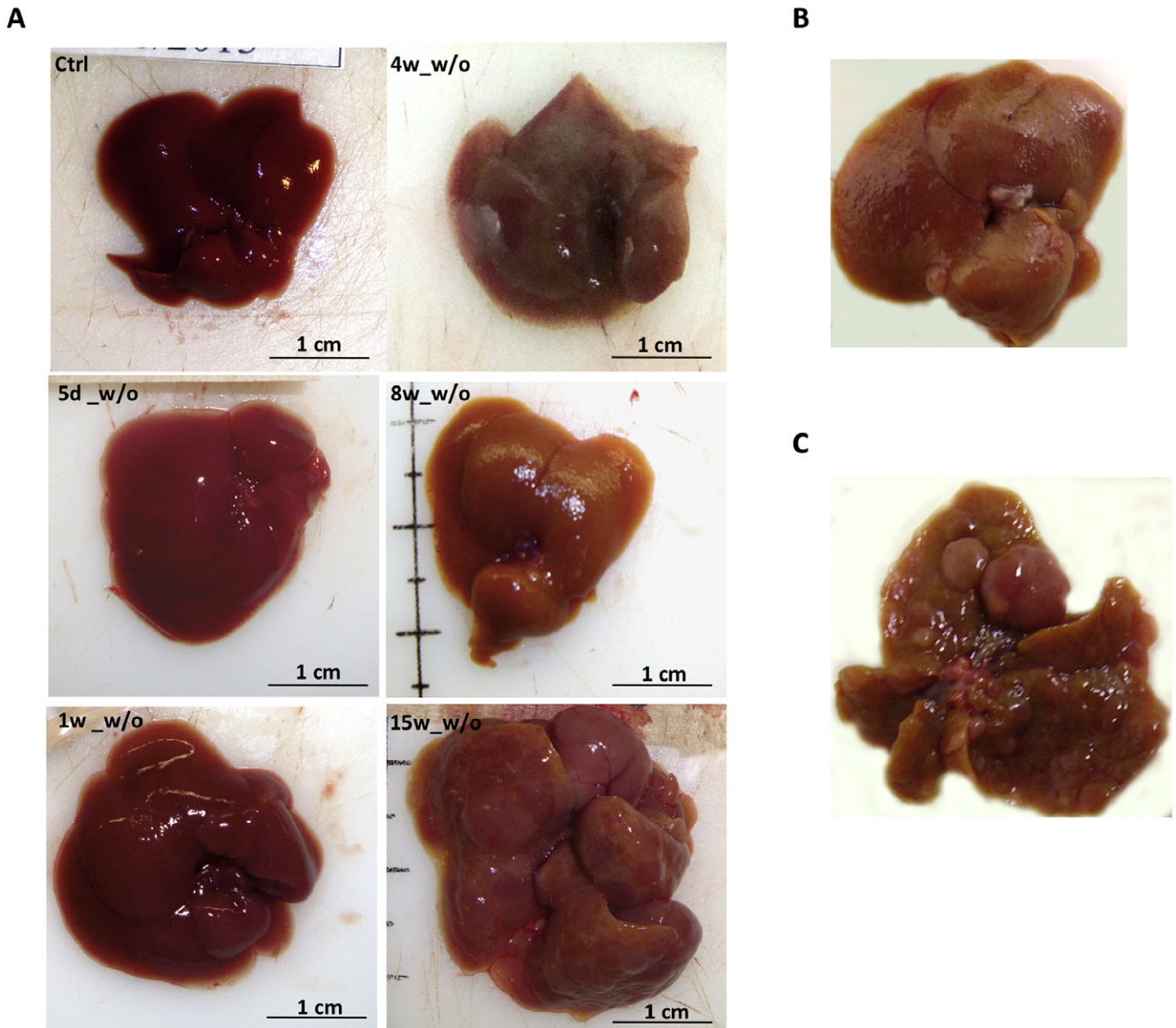


Fig. 3. Representative pictures of whole livers from *fah*^{-/-} mice following NTBC discontinuation. (A) Macroscopic appearance of harvested livers at different time point of 15 weeks withdrawal protocol. Scale bars, 1 cm. (B) Cirrhotic features of liver harvested at 8 weeks post withdrawal. (C) Macronodular appearance of liver harvested at 15 weeks post therapy discontinuation.

(Fig. 5B). Glutamine synthetase, which, in the normal liver, is closely restricted to the few rows of hepatocytes immediately surrounding centrilobular veins, was undetectable in adenoma tissue; its expression was retained in the adjacent peritumoral tissue but its distribution was modified, likely as a result of the architectural disturbances associated with liver injury (Fig. 6). Between liver cell adenomas, the hepatic parenchyma showed major histological changes, as described above, including marked hepatocellular lesions and extensive perisinusoidal fibrosis as shown by Sirius Red and reticulin stains (Fig. 5C).

3.3. Nuclear factor (erythroid-derived 2)-like 2 (Nrf2) is induced in the early phase of NTBC withdrawal

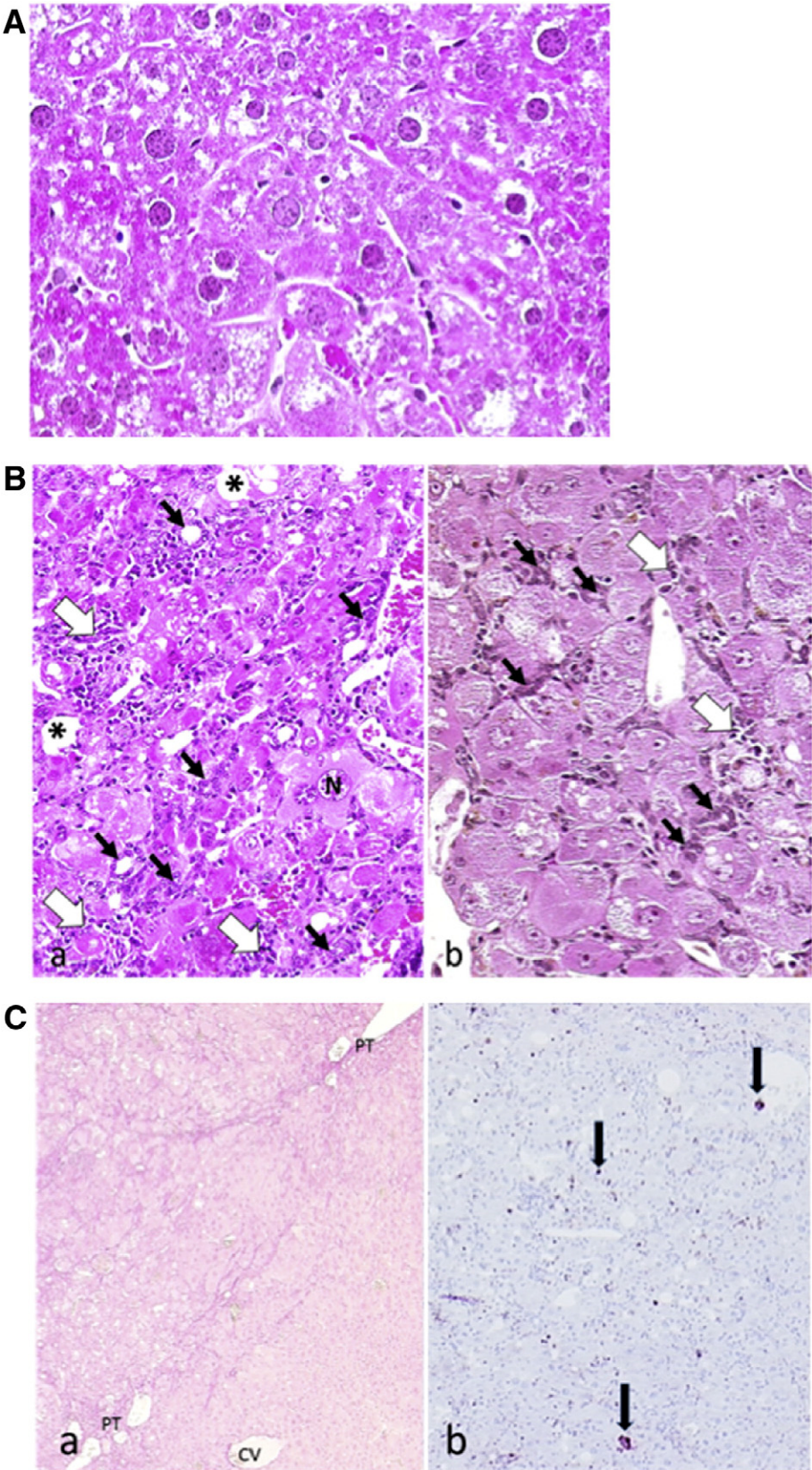
Endogenous oxidative stress enhanced by accumulation of metabolites such as FAA has previously been reported in several studies [10, 12,14]. It has been observed that FAA causes Golgi apparatus disruption

and elicit stress defensive mechanisms by depleting cells of GSH [5,6, 10]. It has been suggested that, Nrf2 could be a critical modulator of FAA-induced toxicity, modulating survival of stressed hepatocytes and delaying tumor development [28]. Thus we examined the levels of Nrf2 protein during the NTBC withdrawal protocol in HT1 stressed mice. The level of Nrf2 was measured on *fah*^{-/-} mice after short-term (from 3 days to 1 week) and long-term (from 4 to 15 weeks) therapy discontinuation ($n = 3-10$; Fig. 2). Expression of Nrf2 occurred soon after NTBC interruption (Fig. 7A,C), with a peak of expression in the acute phase of the tyrosinemic stress (e.g. first week post withdrawal). However an Nrf2 decrease was observed during the HT1 progression. As shown by Western blot analysis (Fig. 7A,C) after four weeks of therapy discontinuation, Nrf2 levels were lower than after one week post-withdrawal, and this trend became more evident after longer therapy interruption (e.g. 8 to 15 weeks after NTBC removal), when liver homogenates presented almost undetectable levels of this protein.

3.4. HO-1 modulation in HT1 disease progression

Nrf2 has been reported to regulate the expression of many cytoprotective enzymes in response to oxidative stress through binding

of antioxidant responsive element (ARE) [37–41]. Among transcriptional targets of Nrf2, heme oxygenase-1 (HO-1) has been the object of many investigations for its multiple roles in molecular signaling. Past studies on the same murine model of HT1, showed an increase of this protein



when mice were subjected to a discontinuation from therapy up to five weeks [6]. This increase was associated to cell stress induced by retrieval from NTBC treatment and was suggested to be part of ER stress response promoted by FAA oxidative damage. Thus we examined HO-1 levels in liver homogenates of *fah*^{-/-} mice following a longer NTBC discontinuation. As observed the expression of HO-1 protein was induced in a time-dependent manner (Fig. 7A,C). Indeed, HO-1 expression was almost absent in NTBC treated *fah*^{-/-} mice but was induced in all the NTBC-withdrawn groups. In particular, the maximal induction of HO-1 was observed after four weeks of therapy discontinuation. In animals withdrawn for longer period (*n* = 4–10) these levels were maintained throughout the entire starvation time even during neoplastic transformation (Figs. 3 and 7A,C). These results confirm and extend our previous observations in the five weeks withdrawal model [6]. Whether this is regulated by translocation of Nrf2 in the nucleus or by other mechanisms has not been measured here. It would certainly be interesting as future perspective to investigate more in details whether HO-1 induction relies or not on Nrf2 nuclear migration during HT1 progression.

3.5. Induction of eukaryotic translation initiation factor 2 α eIF2 α and C/EBP homologous protein-10 (CHOP) in response to NTBC withdrawal

Previous *in vitro* and *in vivo* studies during the first five weeks of NTBC withdrawal showed an activation of eIF2 α as consequence of the oxidative stress elicited by toxic metabolites accumulation in cells lacking FAH activity [6]. Since phosphorylation of the α subunit of eIF2 at serine 51 (p-eIF2 α) is a master regulator of cell adaptation to various forms of stress with implications in cancer growth and proliferation, we then asked whether p-eIF2 α could contribute in sustaining oxidative stress pathways in the HT1 late neoplastic process. As shown in Fig. 7B,D, p-eIF2 α was already induced in mice after five days from NTBC interruption. Moreover, analysis of livers from mice subjected to a longer interruption demonstrated that, p-eIF2 α remains persistently high all through therapy discontinuation (Fig. 7B,D), suggesting an important role for this factor in managing chronic liver injury.

A major target gene of p-eIF2 α is the transcription factor CHOP, which is often up-regulated under stress conditions. Bergeron et al. reported a gain of CHOP protein expression in *fah*^{-/-} mice already after the first week of NTBC withdrawal [6]. Here, Western blot analysis shows a light increase in CHOP expression at four weeks post-withdrawal, with a stronger induction observed in the late stages of HT1 stress when neoplastic lesions are observed (Figs. 3 and 7B,D).

3.6. Sustained liver injury leads to impairment of mitochondrial pathways with progressive cell death resistance

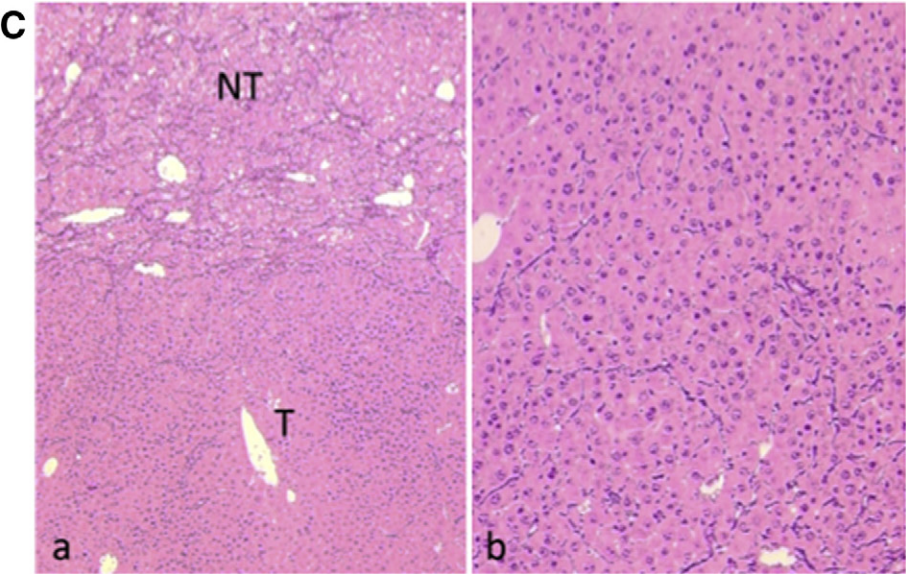
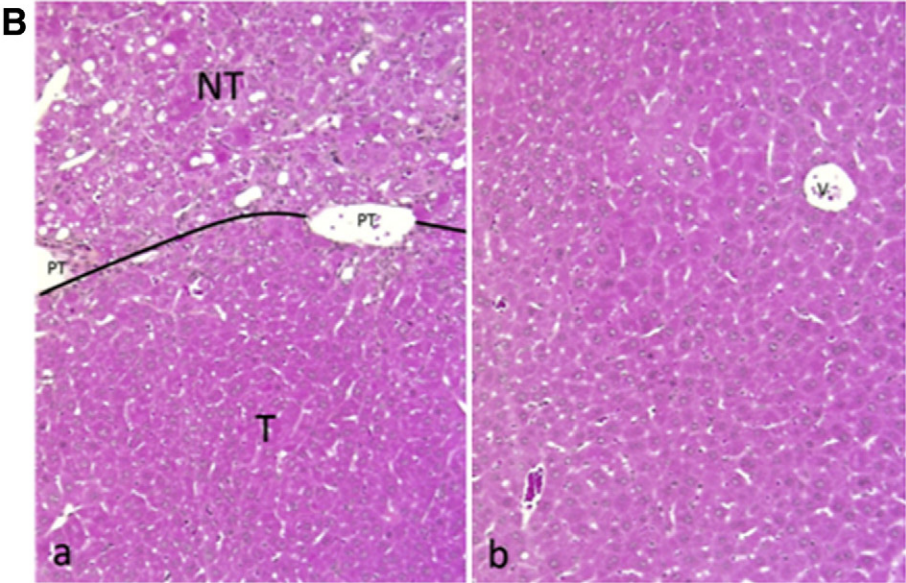
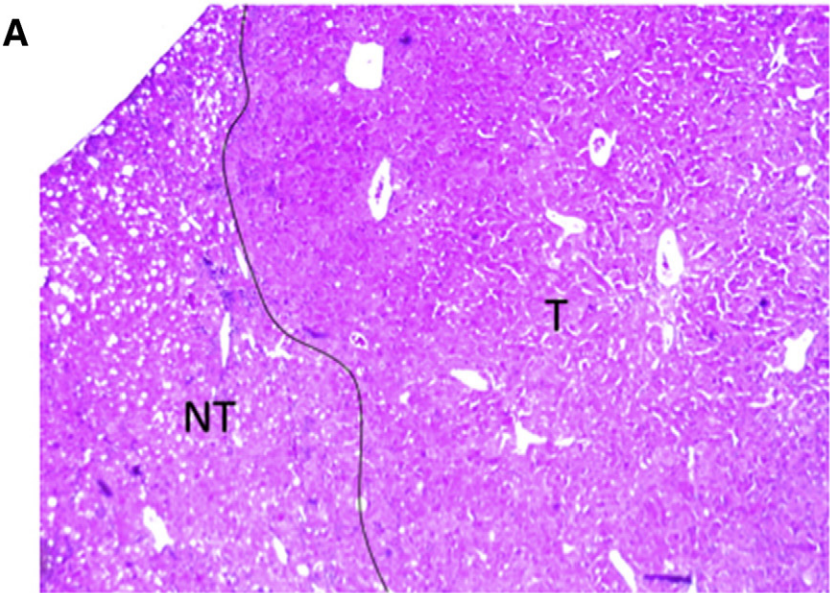
Cell death resistance has been reported to occur rapidly and to affect the majority of hepatocytes in the murine model of HT1 [7,29] but only limited information exists on apoptosis modulation during late HT1 progression. Therefore we investigated the modulation of the BCL-2 family members to better understand how the mitochondrial apoptotic pathways may influence the survival status in liver presenting neoplastic lesions (e.g. 8 to 15 weeks post therapy interruption). As previously

reported [7,8], NTBC withdrawal resulted in approximately 30-fold induction of Bcl-2 protein already in the 5th day post withdrawal, confirming an activation of survival mechanisms during the early HT1 stage (Fig. 8). Bcl-2 levels remained high at 1 and 4 weeks of NTBC discontinuation and returned to normal following longer discontinuation. Moreover, HT1 progression resulted in a sequential increase of phosphorylation levels of Bad, a pro-apoptotic Bcl-2 family member (Fig. 8). Indeed, phosphorylation of Bad appears on S136, five days after therapy discontinuation, while phosphorylation on S112 three weeks later with a peak registered at 8 weeks post-withdrawal (Fig. 8). Phosphorylation at either site should result in loss of the ability of Bad to form hetero-dimer with the survival proteins Bcl-XL or Bcl-2 eliciting the reinforcement of the pro-survival potential and impairing its apoptogenic functions [42]. Contrary to Bcl-2 which is involved in the early stage of HT1, Mcl-1, another pro-survival member of the Bcl-2 family, was induced at 4 weeks of NTBC withdrawal and later, presumably compensating the decreased expression registered for Bcl-2 protein (Fig. 8). Numerous, diverse cell-types have been shown to rely on Mcl-1 for their survival and development [43]. Furthermore Mcl-1 has been reported to block the progression of apoptosis by binding and sequestering the pro-apoptotic proteins Bcl-2-associated protein X (Bax) [43], capable of forming pores in the mitochondrial membrane. Levels of Bax were therefore measured by Western blot analysis and, as shown in Fig. 8, Bax was highly deregulated soon after therapy discontinuation with a marked diminution in the long-term withdrawal.

3.7. Activation of MAPK cascade upon HT1 stress

To further explore the signaling events responsible for death resistance during HT1 progression, we investigated other pathways often activated in cancer cells exposed to chronic stress. Protein kinase B, better known as Akt, was already reported to contribute in apoptosis resistance during HT1 stress [7]; however our new data and others results are indicative of a more complex deregulation involving the cooperation of many others cellular mechanisms. Since, extracellular signal-regulated protein kinase (ERK1/2), a member of the mitogen-activated protein kinase (MAPK) family crucial for regulating cell growth and differentiation in stress condition, is often aberrantly expressed in oncogenesis and since alteration in ERK1/2 activity has been reported in FAA-treated cells [5], we examined expression levels of this protein in *fah*^{-/-} mice subjected to an increasing tyrosinemic stress (i.e. short- and long-term NTBC withdrawal). ERK1/2 activation was assessed using an antibody against the active form, i.e. against phosphorylated ERK1/2 (p-ERK1/2). As shown in Fig. 9, ERK1/2 was significantly activated after four weeks of NTBC removal. No significant variation in total ERK1/2 protein level was observed (Fig. 9A). Levels of mitogen-activated protein kinase (MEK1/2) were then investigated, as it is one of the upstream mediators of ERK1/2 activation in the MAPK pathway. As observed in Western blot analysis, NTBC removal resulted in an increase in phosphorylated MEK1/2 (p-MEK1/2) levels (Fig. 9) at 4 and 8 weeks after therapy interruption, suggesting the involvement of Ras/MEK cascade in ERK1/2 phosphorylation in late events of HT1 progression. Total levels of MEK1/2 protein were not significantly changed through all the HT1 process.

Fig. 4. Histopathological evaluation of post withdrawal liver damage in *fah*^{-/-} mice. Panels are representative of at least three pictures taken per sample of a total number of *n* = 4 mice for each series. Liver lesions observed in 4 months-old *fah*^{-/-} mice treated with NTBC (A) or removed from NTBC therapy during 15 weeks (B, C). (A) *fah*^{-/-} treated mice present mild hepatocellular changes: hepatocytes are enlarged and often contain micro- or macro-vesicular steatosis, they show large dysmorphic nuclei with several well formed nucleoli. HES staining, $\times 350$. (B) *fah*^{-/-} mice withdrawn from NTBC treatment present severe hepatocellular changes. a: Enlarged hepatocytes frequently contain micro- or macro-vacuoles of steatosis (*), dysmorphic nuclei are visible (N) and oval-like cell proliferation is marked. Oval-like cells, identifiable to their large nucleus containing dispersed chromatin and to their well visible cytoplasm, are arranged in small sheets or in tubular structures (black arrows). Inflammatory aggregates, made of loosely grouped small lymphoid cells with dark nuclei and scant cytoplasm, are present (large open arrows). HES staining, $\times 250$. b: At higher magnification, the structures made by oval-like cells are well visible (dark arrows); inflammatory aggregates are frequent (large open arrows). HES staining, $\times 320$. (C) Fibrosis and apoptosis in *fah*^{-/-} mice withdrawn from NTBC treatment. a: Sirius Red staining highlights the presence of thin connective septa running between disorganized hepatocyte plates and extending from portal tracts (PT). CV: centrilobular vein. Sirius Red staining, $\times 170$. b: Immunohistochemical detection of cleaved caspase-3. Several positive cells are visible (arrows). Indirect immunoperoxidase technique, $\times 240$.



3.8. Protein kinase C (PKC) is recruited during oxidative damage in HT1 stress reinforcing cell survival and sustaining neoplastic lesions progression

Induction of the MAPK cascade can be carried out through the activation of PKC, a family of specific serine-/threonine-kinases implicated in a wide variety of cellular responses, including proliferation and regulation of gene expression [44–46]. Moreover during oxidative stress, the PKC family has been proposed to play an important role in the Ca^{2+} mediated signaling of apoptosis by interaction with pro- and anti-apoptotic members of the Bcl-2 family [44,47,48]. Thus, considering our previous observations on Ca^{2+} release in FAA-treated cells [5], and taking into account the results obtained on MAPK cascade and apoptosis signaling, we next assessed the status of the PKC survival pathways considering that it may constitute one of the central nodes in HT1 progression. PKCs levels and its active phosphorylated forms were measured in liver homogenates of mice after different periods of NTBC withdrawal. Interruption of therapy resulted in a progressive induction of PKC isoforms up to 15 weeks (Fig. 10). Immunoblotting results also showed an uneven modulation of total PKC and phosphorylated PKC isoforms levels in the different stages of drug withdrawal (Fig. 10B). This result may indicate that preferential phosphorylation of some isoforms may occur in the development and progression of the HT1 liver pathology.

3.9. Transcriptomic analysis in liver of *fah*^{−/−} mice under long term NTBC withdrawal reveals cluster of genes involved in cancer progression

Liver injury in both HT1-affected mice and HT1 patients has been associated with alteration of transcripts related to oxidative stress, detoxification enzymes and GSH-metabolism related proteins [14,28,33]. In order to identify genes involved in the chronic stress induced during HT1, we performed microarray profiling in mice after 7–8 weeks of drug starvation, ($n = 4$), using *fah*^{−/−} NTBC-treated mice as control ($n = 4$). This time point was characterized by significant modulation of many signaling cascades (Figs. 7–10) and appearance of neoplastic changes (Figs. 3–6).

Interestingly, 32 genes related to GSH metabolism and oxidative stress were up-regulated following 8 weeks of NTBC discontinuation, reflecting a strong transcriptional response to oxidative stress in the progression of the chronic HT1 stage (Table 1). In accordance with immunoblotting experiments (Fig. 7A, C), HO-1 transcript (*HMOX*) was up-regulated by more than 5 fold (Table 1). Further integration of differently regulated genes into specific regulatory signaling networks was carried out using Ingenuity Pathway Analysis (Fig. 11A). According to these data, we clustered among over 3000 genes differently regulated. The most significant enriched biological processes and networks were those involved in cellular growth and proliferation, cell survival, inflammatory response, hepatic fibrosis and hepatic stellate cells (HSCs) activation, organismal injury and cancer (Fig. 11A).

Throughout the top overexpressed molecules we found genes widely correlated in literature with the oncogenic process (Fig. 11B). Among these, alpha-fetoprotein (AFP), one of the most widely used biomarker for HCC surveillance [49], was also tested by Western blot analysis, showing up to 35-fold higher expression in long-term NTBC withdrawal (Fig. 12).

4. Discussion

Chronic liver injury inflicted by HT1 has been associated with the highest risk of HCC of any human disease [29,50]. Although NTBC

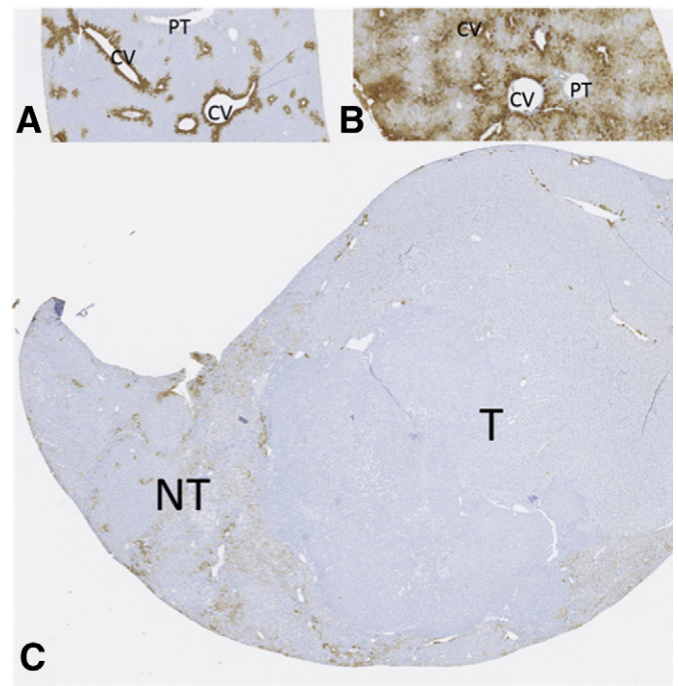


Fig. 6. Glutamine synthetase distribution is altered following NTBC withdrawal. Glutamine synthetase (GS) immunodetection in normal mouse liver (A), diseased liver from 4 months-old *fah*^{−/−} mouse withdrawn from NTBC during 15 weeks (B), and in a liver cell adenoma (C). A) In the normal liver, GS is restricted to the few rows of hepatocytes surrounding centrilobular veins (CV) ($\times 190$). B) In diseased liver, GS expression is retained but the distribution is markedly enlarged and disorganized ($\times 190$). C) In liver cell adenoma (T), no expression is detectable in contrast to adjacent peritumoral liver (NT) ($\times 110$). PT: portal tract.

therapy has improved the expectancy of life in HT1 patients since its introduction in 1992 [51–53], the risk of developing HCC is still a serious threat for improving the management of this devastating disease.

Histological evidences shows that *fah*^{−/−} mice, continuously under therapy since mother pregnancy, experience signs of stress under basal conditions, suggesting that NTBC treatment does not fully normalize HT1-induced alterations as already suggested by others [24,33]. This may indicate that HPPD has some remaining activity even under NTBC treatment and that although the drug reduces FAA, MAA and SA accumulation, their production may not be completely suppressed. As consequence a subtle and continuous damage induced by these toxic metabolites could expose HT1 patients to the risk of developing HCC as long-term complication. In the mouse model, the severity of this pathological condition is evident soon after *fah*^{−/−} mice are removed from therapy, when they start to manifest a progressive degradation of the normal physiology. Up to now the rapidly lethal phenotype induced by drug withdrawal in the *fah*^{−/−} mice represented a limitation for long-term observation of the HT1 progression, since the median mice survival was between four and five weeks after therapy interruption (Fig. 2B). Herein, we modified our experimental protocol supplementing the mice diet with water soaked food to overcome the dehydration and gastro-intestinal problems that characterize the acute HT1 phenotype in *fah*^{−/−} mice. This expedient resulted in a longer survival of mice under experimental protocol allowing an extension of our observations up to 15 weeks post drug removal. Histological analysis

Fig. 5. Presence of liver cell adenoma in *fah*^{−/−} mice withdrawn from NTBC during 15 weeks. Panels are representative of at least three pictures taken per sample of a total number of $n = 4$ mice for each series. (A) Low magnification of a liver cell adenoma presenting as a well-demarcated, expansive nodule (T, tumor, NT, non tumoral liver). HES staining, $\times 150$. (B) High magnifications of the periphery (a) and center (b) of a liver cell adenoma; the histological appearance of the adenoma (T) is very different from that of the adjacent peritumoral tissue (NT). Tumor cells are monomorphic, with an increased nucleo-cytoplasmic ratio and a basophilic cytoplasm. They are arranged into thick plates; there is no cell atypia and no visible mitosis; portal tracts (PT) are visible only in the adjacent liver; only venous structures (V) are present within the tumor tissue. HES staining, $\times 220$. (C) At low magnification (a), reticulin stain shows the scarcity of reticulin network in liver cell adenoma tissue (T) as contrast to adjacent non tumoral liver (NT). At higher magnification (b), only scattered reticulin fibers are visible within adenoma tissue; the reticulin network is poor and highly disorganized. Reticulin staining, $\times 220$.

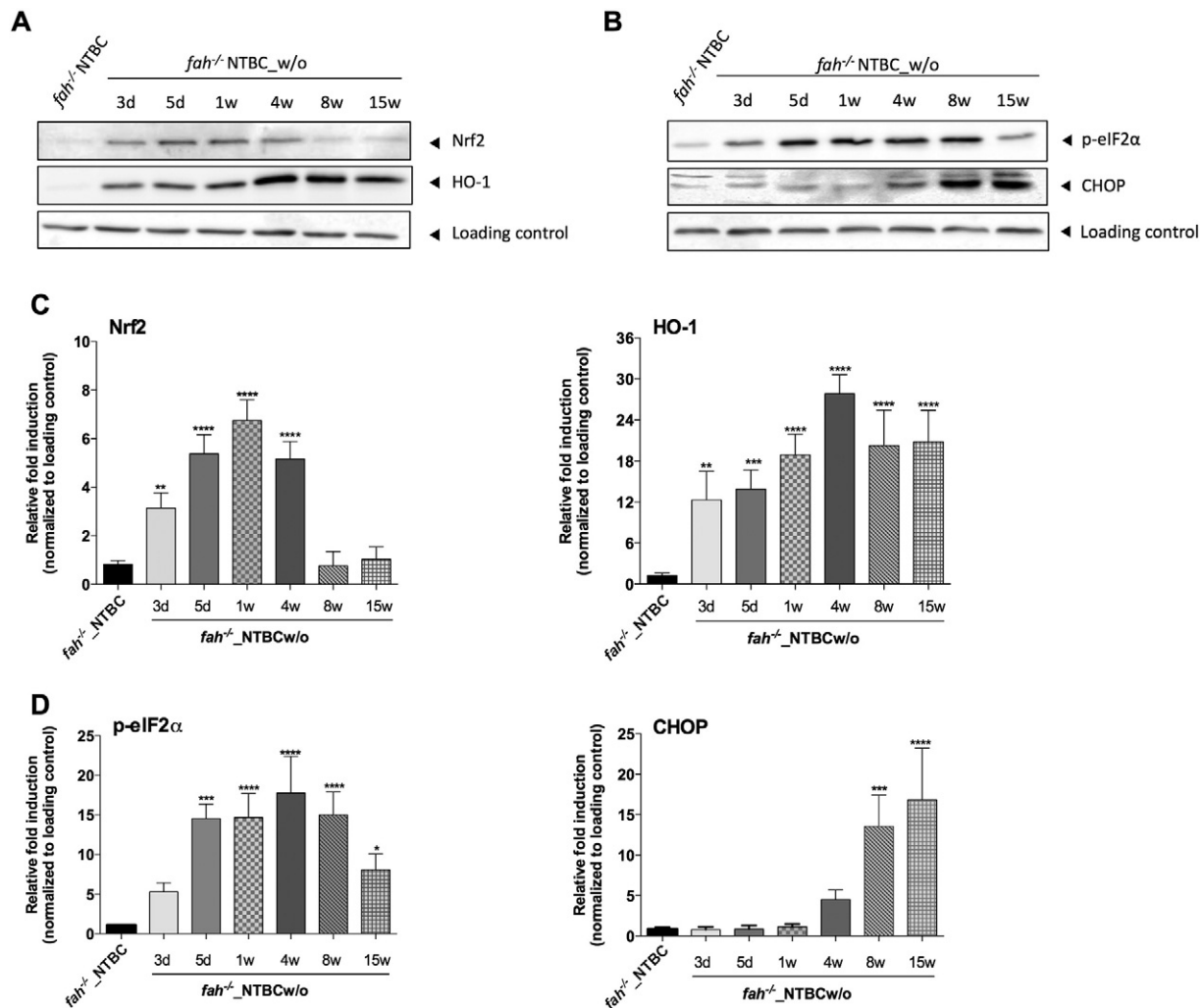


Fig. 7. Effect of NTBC withdrawal on ER stress response proteins. Protein expression levels of Nrf2 (A), HO-1 (A), p-eIF2α (B) and CHOP (B) following NTBC interruption. One mouse is presented per group. (C, D) Bar graphs showing quantification of the expression level of each protein compared with the expression levels of the control group (NTBC-treated) and normalized to the loading control (HSP60). Data are expressed as means \pm s.d. (n = 4). Western blots are representative of at least four independent experiments. * $p < 0.05$, ** $p < 0.01$, *** $p < 0.001$ and **** $p < 0.0001$.

carried out on livers of mice harvested at different stage from therapy interruption, showed a progressive and constant liver degeneration, under drug starvation, accompanied by activation of stress and survival pathways with neoplastic lesions in 100% mice under experimentation. Altogether, the immunoblotting experiments suggest that HT1 progression can be divided in two-phases. It was already shown that the half-life of NTBC in mouse plasma is 54 h and that HPPD is completely inhibited only in the 3 first days following a single-dose of NTBC [32]. However it was also shown that a small portion of NTBC is retained in the liver up to 7 days after NTBC uptake, preventing the full recovery of HPPD activity before the first week post-withdrawal [32]. Therefore, the differences observed between the early and late events of HT1 may be in part linked to a different level of HT1-toxic metabolites accumulation. Furthermore, immunoblotting results revealed the involvement of ER key factors such as Nrf2 and eIF2α since the early stage of HT1-induced oxidative damage.

Nrf2 can be activated by different mechanisms such as oxidation of its sequestering partner kelch-like ECH-associated protein 1 (Keap1) or directly by PERK [54]. Another not yet tested possibility could be by the direct interaction of FAA with sulfhydryl groups of Keap1 since Nrf2 levels increased immediately after NTBC withdrawal in liver homogenates of *fah*^{-/-} mice. However, Nrf2 levels decrease in the long-term therapy interruption. Since Nrf2 has been shown to play a crucial

role in preventing liver fibrosis [28,55] and *Nrf2*^{-/-} mice were reported to suffer an abnormality in lipid metabolism [56,57], the decreased expression of this transcription factor in *fah*^{-/-} mice might then be associated with an impairment of hepatic regeneration and lipid homeostasis in the advanced stage of HT1 disease.

Analyses on *fah*^{-/-} mice revealed that NTBC discontinuation elicits significant eIF2α activation soon after drug interruption. eIF2α phosphorylation is known to attenuate global protein synthesis and ER overload by misfolded proteins, which lowers energy expenditure and facilitates reprogramming of gene expression to remediate stress damage [58,59]. For example, increased p-eIF2α mediates expression of genes involved in adaptation to amino acid starvation and alleviation of oxidative damage from nutrient deprivation [60,61]. It is possible that stressed hepatocytes use the anti-oxidant function of p-eIF2α for inducing transcription of genes involved in the import of thiol-containing amino acids and glutathione biosynthesis, as means to counteract the continuous oxidative insults elicited by FAA and MAA overproduction. Moreover, p-eIF2α was suggested to increase the activation of CHOP in condition of cellular damage coupled with metabolic stress [62].

In the *fah*^{-/-} model, CHOP was induced from the eighth week post therapy interruption. CHOP is a stress-regulated transcription factor that influences ER function and cell viability through its actions on

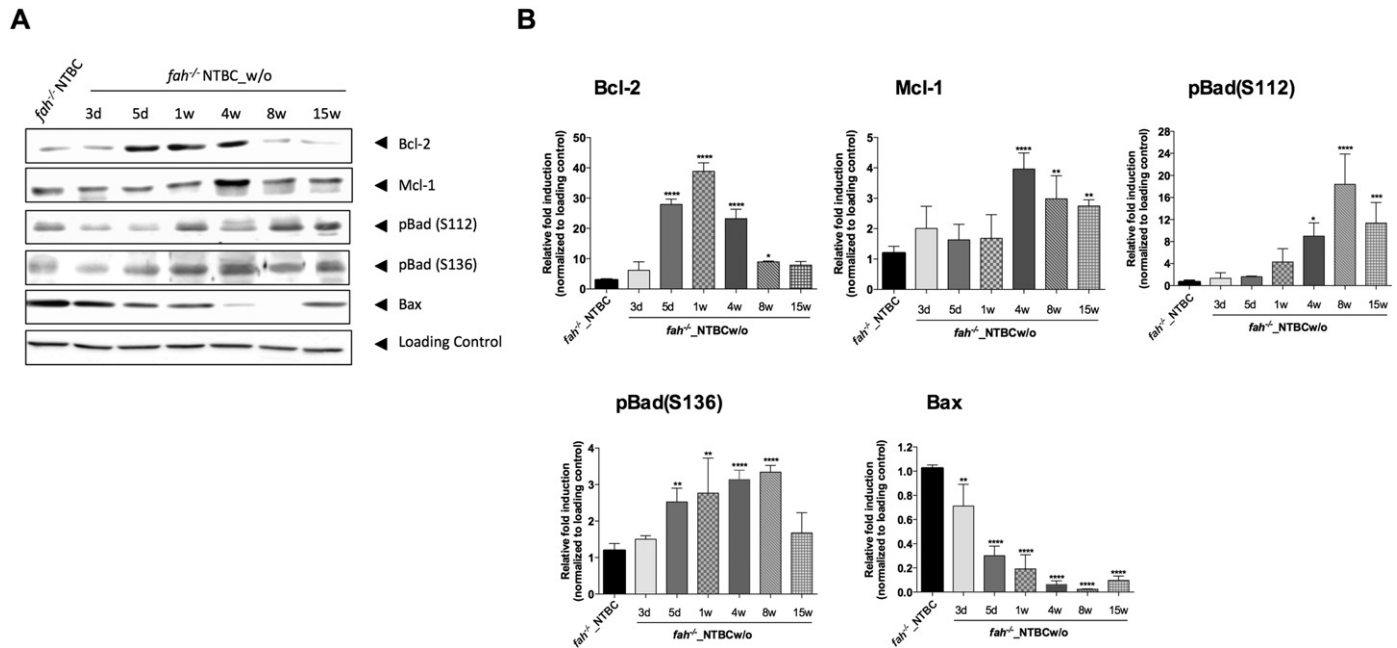


Fig. 8. Mitochondrial apoptotic pathway during HT1 progression. (A) Immunoblot analysis showing mitochondrial proteins of the apoptotic pathway from a representative mouse for each group (n = 4). Phosphorylation is indicative of a loss of function in analyzed proteins. (B) Bar graphs showing quantification of the expression level of each protein compared with the expression levels of the control group (NTBC-treated) and normalized to the loading control (HSP60). Data are expressed as means \pm s.d. (n = 4). Western blots are representative of four independent experiments of a total number of n = 4 mice for each series. * $p < 0.05$, ** $p < 0.01$, *** $p < 0.001$ and **** $p < 0.0001$.

target genes involved in protein synthesis and oxidative protein folding [63,64]. While it is known to mediate apoptosis in response to ER stress and is considered as a sentinel for the failure of cells to adapt to chronic stress [65–68], several studies hint at an oncogenic role of CHOP in certain tumor environments [69–71]. Indeed, CHOP was hypothesized to contribute to the pathogenesis of HCC *in vivo* by promoting apoptosis, inflammation, fibrosis and compensatory proliferation [72]. Therefore, activation of CHOP in the late stage of HT1 hepatic dysfunction could worsen the inflammatory response and stimulates HSCs activation and fibrosis, enhancing compensatory hepatocyte proliferation and sustaining liver tumorigenesis.

In such context of multifaceted interactions addressed to counteract an overall imbalance of the homeostatic equilibrium, cellular defense mechanisms orchestrate the execution of the antioxidant response

element-dependent gene transcription program. The complexity of HO-1 regulation is illustrated by the multiplicity of signaling cascades that are involved in the regulation of this gene, including PKCs and MAPKs [73], and that are highly represented in HT1 progression. Many recent evidences suggest a role for HO-1 in promoting cancer, since its activity has closely been related to growth, apoptosis, angiogenesis, invasiveness, and metastasis of solid tumors [74,75]. Previous results already reported its involvement in liver injury induced by HT1 stress, however its role was not investigated as part of the pathways involved in liver tumorigenesis [6]. Here, the high protein levels of this factor found in the late HT1 stage (Fig. 7A,C), might indicate that it plays a crucial role not just in defense against oxidative stress induced by HT1 toxic metabolites but also in promoting survival of proliferating cells. Moreover, HO-1 induction results in production of

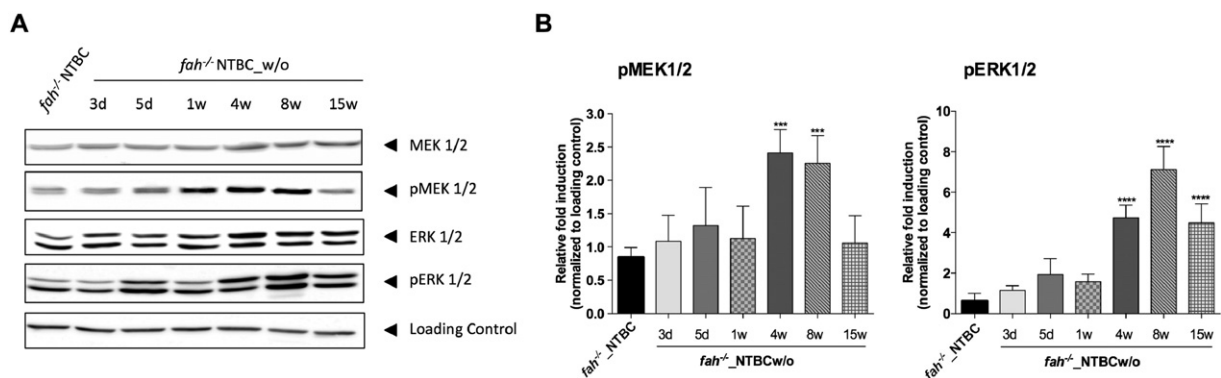


Fig. 9. MEK/ERK protein expression level in *fah*^{-/-} withdrawn mice. (A) Immunoblot analysis show data from a representative mouse for each group (n = 4). Phosphorylated form and endogenous total level were analyzed to evaluate level of activation of each protein. (B) Bar graphs showing quantification of the expression level of pMEK1/2 and pERK1/2 compared with the expression levels of the control group (NTBC-treated) and normalized to the loading control (HSP60). Data are expressed as means \pm s.d. (n = 4). Levels of endogenous MEK1/2 and ERK1/2 did not show any significant variation and are therefore not shown. Western blots are representative of four independent experiments of a total number of n = 4 mice for each series. *** $p < 0.001$ and **** $p < 0.0001$.

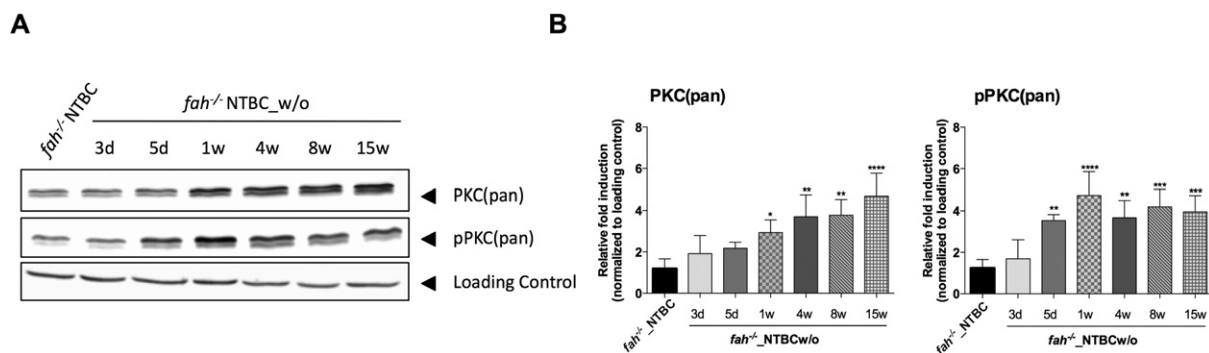


Fig. 10. PKC expression levels in 15 weeks post withdrawal protocol. (A) Immunoblot analysis of phosphorylated forms of total PKC and endogenous PKC levels. Images show representative data from individual mouse in each group (n = 4). (B) Bar graphs showing quantification of the expression level of each protein compared with the expression levels of the control group (NTBC-treated) and normalized to the loading control (HSP60). Data are expressed as means ± s.d. (n = 4). Western blots are representative of four independent experiments of a total number of n = 4 mice for each series. *p < 0.05, **p < 0.01, ***p < 0.001 and ****p < 0.0001.

carbon monoxide (CO), that has been reported to reduce the phosphofructokinase-1 activity, a rate-limiting glycolytic enzyme. This mechanism shifting glucose utilization from glycolysis toward the pentose phosphate pathway would determine directional glucose utilization to ensure resistance against oxidative stress for cancer cell survival [76]. Increasing the intracellular use of glucose could then contribute in decreasing blood sugar levels, a phenomenon observed in HT1-affected individuals [19] and in animal models [7,77]. Most cancer cells exhibit increased glycolysis and use this metabolic pathway for generation of ATP as a main source of their energy supply. This

phenomenon is known as the Warburg effect and is considered as one of the most fundamental metabolic alterations during malignant transformation. Biochemical and molecular studies suggest several possible mechanisms by which this metabolic alteration may evolve during cancer development. These mechanisms include mitochondrial defects and malfunction. Mitochondria and ER interact physically and functionally to form endomembrane networks that constitute a complex connection in regulating several signaling mechanisms. The molecular foundations of this crosstalk are diverse, and Ca^{2+} is one of the most important signals that these organelles use for communication [78]. Since disturbance of ER homeostasis in HT1 stress has been shown to result in functional alterations of Golgi organelles and mobilization of intracellular Ca^{2+} reservoirs [5], it is possible that the observed impairment of mitochondrial pathways is a consequence of this perturbation. Indeed, anti-apoptotic and pro-apoptotic members of the Bcl-2 family have been shown to be fine sensors of Ca^{2+} homeostasis controlling cell death induced by agent known to trigger ER stress [79–81]. Here we show that modulation of these pathways occurs not just in the initial phase of HT1 stress, but instead mitochondrial dysfunction seems to be also involved in the late stage when neoplastic lesions are observed. The rise in intracellular Ca^{2+} level is furthermore linked to activation of multiple signaling modulators critically regulated by Ca^{2+} conductance like several PKC isoforms and MAPK/ERKs. Because of their key roles in cell signaling, PKC isoforms have been the object of many studies as potential therapeutic target for several diseases [82,83]. Substantial information obtained from animal models indicates that during cancer cell proliferation, PKC isoforms stimulate survival or proliferation associated signaling pathways, such as Ras/Raf/MEK/ERK or PI3K/Akt/mTOR pathways, but suppress the expression of cancer suppressor-associated or apoptotic signals such as caspase cascade or Bax subfamily [82]. Here we show that hepatic damage following FAA/MAA/SA toxic actions results in an induction of PKC signaling pathway. Further studies are needed to elucidate the involvement of the different PKC isoforms in HT1 dysfunction and to establish whether the mechanism of PKC activation resides on direct Ca^{2+} mobilization or if it is more dependent on receptor mediated pathways (i.e. tyrosine-kinase receptor, RTK and G-protein-coupled receptor, GPCR). Nonetheless, it seems appropriate to suggest that PKC is involved in HT1 progression and that through target protein phosphorylation PKC isoforms, directly or indirectly, participate in activation of several signaling cascade sustaining cancer development in HT1 patients. Among the most recognized pathways downstream PKC activation in cancer environment, an important role has been attributed to MAPK/ERK signaling cascade [84,85]. RAS/RAF/MEK pathway is activated in more than 30% of human cancers and ERK phosphorylation has been associated with transcriptional mutagenesis causing tumor development in mammalian cells [86,87]. Induction of this pathway during the pathological progression of HT1 phenotype

Table 1
Top up-regulated genes involved in GSH metabolism and oxidative stress response in 8 weeks post withdrawal mice (Fold change >2, p < 0.001).

Symbol	Description	Fold change
ATF3	Activating transcription factor 3	4
CYGB	Cytoglobin	2.56
DHCR24	24-Dehydrocholesterol reductase	2.7
ERO1L	ERO1-like (S. cerevisiae)	3.773
G6PD2	Glucose-6-phosphate dehydrogenase 2	4.86
G6PDX	Glucose-6-phosphate dehydrogenase X-linked	8.01
GCLC	Glutamate-cysteine ligase, catalytic subunit	6.07
GGT1	Gamma-glutamyltransferase 1	10.52
GPX2	Glutathione peroxidase 2	9.28
GPX3	Glutathione peroxidase 3	3.241
GPX4	Glutathione peroxidase 4	2.327
GPX7	Glutathione peroxidase 7	3.4
GSR	Mitochondrial glutathione reductase	4
GSTA1	Glutathione S-transferase, alpha 1 (Ya)	3.94
GSTA2	Glutathione S-transferase, alpha 2 (Ya)	2.74
GSTM2	Glutathione S-transferase, mu 2	5.408
HIF1A	Hypoxia inducible factor 1, alpha subunit (basic helix-loop-helix transcription factor)	2.18
HMOX	Heme oxygenase 1	5.98
HSF2	Heat shock factor 2	3.3
MGST2	Microsomal glutathione S-transferase 2	9.946
MGST3	Microsomal glutathione S-transferase 3	7.24
MMP14	Matrix metalloproteinase 14 (membrane-inserted)	3.34
NQO1	NAD(P)H dehydrogenase, quinone 1	5.85
PERK	Eukaryotic translation initiation factor 2-alpha kinase 3	2.348
PGD	Phosphogluconate dehydrogenase	3.34
PTGS2	Prostaglandin-endoperoxide synthase 2 (prostaglandin G/H synthase and cyclooxygenase)	2.4
RRM2	Ribonucleotide reductase M2	2.87
RRM2B	Ribonucleotide reductase M2 B (TP53 inducible)	2.7
SLC7A11	Solute carrier family 7, member 11	8.4
SRXN1	Sulfiredoxin 1	4.482
TXNRD1	Thioredoxin reductase 1	2.324
UCP2	Uncoupling protein 2 (mitochondrial, proton carrier)	3.2

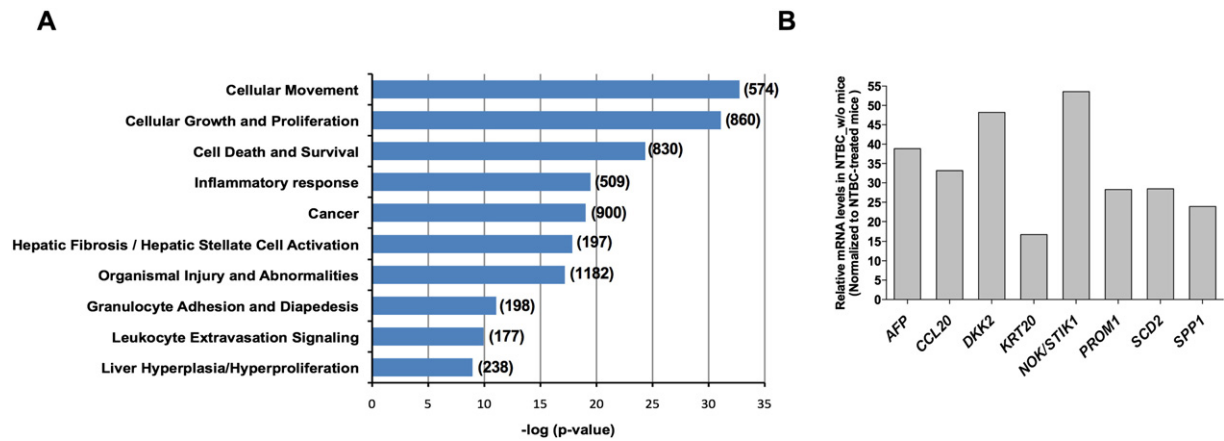


Fig. 11. Gene expression analysis in *fah*^{-/-} mice withdrawn from NTBC. Microarray analysis was performed on 4 mice withdrawn from NTBC for 7–8 weeks to identify gene involved in HT1 progression. (A) Functional analysis of the top deregulated genes in liver, classified according to Ingenuity Pathway Analysis (IPA). *P* values were corrected for multiple testing by the Benjamini–Hochberg method and calculated by IPA software. Values in parentheses indicate the number of genes in each category. (B) Top overexpressed genes related to cancer in literature. Values of *fah*^{-/-} untreated mice were normalized to *fah*^{-/-} mice under NTBC treatment (*n* = 4). Data are expressed as mean of two experiences in a single scan, each sample is representative of a comparison between two pools of four mice each. *p* < 0.05 was considered significant.

might indicate further involvement of this cascade in the complex framework that characterizes development and progression of this pathological condition.

5. Conclusion

By supplementing *fah*^{-/-} mice diet with water soaked food we were able to prolong their lifespan by at least three times, enabling the study of molecular changes associated with HT1 progression up to 15 weeks following NTBC interruption. Our results show that the progression of HT1 disease can be divided in two events: early and late. The early stage of HT1 is characterized by the activation of Nrf2, HO-1, eIF2 α and PKC in response to the accumulation of the toxic metabolites associated with HT1 since it is triggered as soon as 3 days following NTBC interruption. This early stage is also characterized by the strong induction of Bcl-2 and the inhibition of Bad and Bax. The late stage of the disease is associated with the addition of other anti-apoptotic changes as well as with induction of CHOP, MEK and ERK. These changes were accompanied with a sustained induction of HO-1 and eIF2 α and most importantly with the robust induction of AFP. Therefore HT1 progression is characterized by a rapid stress response initiated to cope with damages induced by the accumulation of toxic metabolites and a late stage where perturbation of cellular homeostasis results in the integration of cell death resistance and proliferation mechanisms, promoting neoplastic

lesions and tumor growth. In such context proliferating cells seem to take advantage of ER increased activity to facilitate the folding, assembling and transport of membrane and secretory proteins necessary to their growth and expansion.

Author contribution

FA and RMT conceived the study and designed the experiments. RMT supervised the project, directed the work and edited the manuscript with GM. FA interpreted the data and wrote the paper with GM. FA, VR and DO performed the experiments. GM gave technical support and conceptual advice. JYS and NG carried out histological examination of tissues.

Conflict of interests

The authors declare they have no conflict of interests pending.

Transparency document

The [Transparency document](#) associated with this article can be found, in the online version.

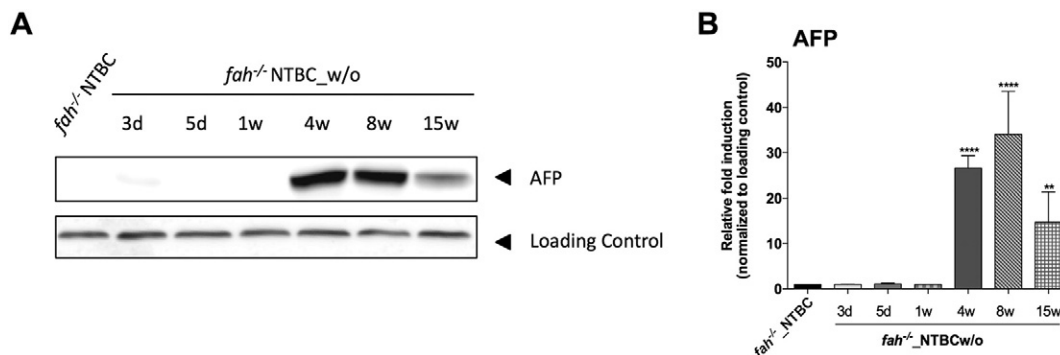


Fig. 12. Analysis of AFP expression in *fah*^{-/-} mice following NTBC discontinuation. (A) Representative immunoblot of AFP protein expression level from individual mouse in each group. (B) Bar graphs showing quantification of AFP expression level compared to expression levels of the control group (NTBC-treated) and normalized to the loading control (HSP60). Data are expressed as means \pm s.d. (*n* = 4). Western blots are representative of four independent experiments. ** *p* < 0.01 and **** *p* < 0.0001.

Acknowledgments

This work was supported by grants from the CIHR (RMT, MOP-86566), the Fondation du Grand Défi Pierre Lavoie (RMT) and postdoctoral (FA) and doctoral (DO) fellowships from PROTEO, and studentships from PROTEO and CORAMH (Corporation de recherche et d'action sur les maladies héréditaires) to VR. We are very thankful to Dr. Linda Hendershot (St. Jude Children's Research Hospital, Memphis, TN, USA) for her comments and advices on the manuscript.

References

- [1] R.M. Tanguay, R. Jorquera, J. Poudrier, M. St-Louis, Tyrosine and its catabolites: from disease to cancer, *Acta Biochim. Pol.* 43 (1996) 209–216.
- [2] G.A. Mitchell, M. Grompe, H. Lambert, R.M. Tanguay, Hypertyrosinemia, in: C. Scriver, A. Beaudet, W.S.J. Sly, D. Valle (Eds.), *The Metabolic and Molecular Bases of Inherited Diseases*, McGrawHill II, New York 2001, pp. 1777–1805.
- [3] P.A. Russo, G.A. Mitchell, R.M. Tanguay, Tyrosinemia: a review, *Pediatr. Dev. Pathol.* 4 (2001) 212–221.
- [4] M. Grompe, The pathophysiology and treatment of hereditary tyrosinemia type 1, *Semin. Liver Dis.* 21 (2001) 563–571.
- [5] R. Jorquera, R.M. Tanguay, Fumarylacetoacetate, the metabolite accumulating in hereditary tyrosinemia, activates the ERK pathway and induces mitotic abnormalities and genomic instability, *Hum. Mol. Genet.* 10 (2001) 1741–1752.
- [6] A. Bergeron, R. Jorquera, D. Orejuela, R.M. Tanguay, Involvement of endoplasmic reticulum stress in hereditary tyrosinemia type I, *J. Biol. Chem.* 281 (2006) 5329–5334.
- [7] D. Orejuela, R. Jorquera, A. Bergeron, M.J. Finegold, R.M. Tanguay, Hepatic stress in hereditary tyrosinemia type I (HT1) activates the AKT survival pathway in the fah^{-/-} knockout mice model, *J. Hepatol.* 48 (2008) 308–317.
- [8] F. Angileri, G. Morrow, V. Roy, D. Orejuela, R.M. Tanguay, Heat shock response associated with hepatocarcinogenesis in a murine model of hereditary tyrosinemia type I, *Cancers (Basel)* 6 (2014) 998–1019.
- [9] F.J. van Spronsen, Y. Thomasse, G.P. Smit, J.V. Leonard, P.T. Clayton, V. Fidler, R. Berger, H.S. Heymans, Hereditary tyrosinemia type I: a new clinical classification with difference in prognosis on dietary treatment, *Hepatology* 20 (1994) 1187–1191.
- [10] R. Jorquera, R.M. Tanguay, The mutagenicity of the tyrosine metabolite, fumarylacetoacetate, is enhanced by glutathione depletion, *Biochem. Biophys. Res. Commun.* 232 (1997) 42–48(47).
- [11] R. Jorquera, R.M. Tanguay, Cyclin B-dependent kinase and caspase-1 activation precedes mitochondrial dysfunction in fumarylacetoacetate-induced apoptosis, *FASEB J.* 13 (1999) 2284–2298.
- [12] S. Kubo, M. Sun, M. Miyahara, K. Umeyama, K. Urakami, T. Yamamoto, C. Jakobs, I. Matsuda, F. Endo, Hepatocyte injury in tyrosinemia type 1 is induced by fumarylacetoacetate and is inhibited by caspase inhibitors, *Proc. Natl. Acad. Sci. U. S. A.* 95 (1998) 9552–9557.
- [13] S. Manabe, S. Sassa, A. Kappas, Hereditary tyrosinemia. Formation of succinylacetone-amino acid adducts, *J. Exp. Med.* 162 (1985) 1060–1074.
- [14] M.Z. Dieter, S.L. Freshwater, M.L. Miller, H.G. Shertzer, T.P. Dalton, D.W. Nebert, Pharmacological rescue of the 14CoS/14CoS mouse: hepatocyte apoptosis is likely caused by endogenous oxidative stress, *Free Radic. Biol. Med.* 35 (2003) 351–367.
- [15] H.S. Edwards, J.C. Bremner, I.J. Stratford, Induction of hypoxia in the KHT sarcoma by tumour necrosis factor and flavone acetic acid, *Int. J. Radiat. Biol.* 59 (1991) 419–432.
- [16] R.S. Galhardo, P.J. Hastings, S.M. Rosenberg, Mutation as a stress response and the regulation of evolvability, *Crit. Rev. Biochem. Mol. Biol.* 42 (2007) 399–435.
- [17] H.B. Lantum, D.C. Liebler, P.G. Board, M.W. Anders, Alkylation and inactivation of human glutathione transferase zeta (hGSTZ1-1) by maleylacetone and fumarylacetone, *Chem. Res. Toxicol.* 15 (2002) 707–716.
- [18] L. Sniderman King, C. Trahms, C.R. Scott, Tyrosinemia type 1, in: Pagon RA, Adam MP, Ardinger HH, et al., editors, *University of Washington, Seattle, GeneReviews™* [Internet]. 2006 Jul 24 [Updated 2014 Jul 17]. (Available from: <http://www.ncbi.nlm.nih.gov/books/NBK1515>)
- [19] C. de Laet, C. Dionisi-Vici, J.V. Leonard, P. McKiernan, G. Mitchell, L. Monti, H.O. de Baulny, G. Pintos-Morell, U. Spiekert, Recommendations for the management of tyrosinemia type 1, *Orphanet J. Rare Dis.* 8 (2013) 8.
- [20] C. Dionisi-Vici, C. Boglino, M. Marcellini, L. De Sio, A. Inserra, G. Cotugno, G.D.A. Sabetta, Tyrosinemia type 1 with early metastatic hepatocellular carcinoma: combined treatment with NTBC, chemotherapy and surgical mass removal, *J. Inher. Metab. Dis.* 20 (Suppl. 1) (1997) 3.
- [21] E. Holme, S. Lindstedt, Nontransplant treatment of tyrosinemia, *Clin. Liver Dis.* 4 (2000) 805–814.
- [22] J. Ros Viladoms, M.A. Vilaseca Busca, N. Lambruschini Ferri, A. Mas Comas, E. Gonzalez Pascual, E. Holme, Evolution of a case of tyrosinemia type I treated with NTBC, *An. Esp. Pediatr.* 54 (2001) 305–309.
- [23] M. Grompe, S. Lindstedt, M. al-Dhalimy, N.G. Kennaway, J. Papaconstantinou, C.A. Torres-Ramos, C.N. Ou, M. Finegold, Pharmacological correction of neonatal lethal hepatic dysfunction in a murine model of hereditary tyrosinemia type I, *Nat. Genet.* 10 (1995) 453–460.
- [24] M. Al-Dhalimy, K. Overturn, M. Finegold, M. Grompe, Long-term therapy with NTBC and tyrosine-restricted diet in a murine model of hereditary tyrosinemia type I, *Mol. Genet. Metab.* 75 (2002) 38–45.
- [25] M. Grompe, M. al-Dhalimy, M. Finegold, C.N. Ou, T. Burlingame, N.G. Kennaway, P. Soriano, Loss of fumarylacetoacetate hydrolase is responsible for the neonatal hepatic dysfunction phenotype of lethal albino mice, *Genes Dev.* 7 (1993) 2298–2307.
- [26] B. Thoolen, R.R. Maronpot, T. Harada, A. Nyska, C. Rousseaux, T. Nolte, D.E. Malarkey, W. Kaufmann, K. Kuttler, U. Deschl, D. Nakae, R. Gregson, M.P. Vinlove, A.E. Brix, B. Singh, F. Belpoggi, J.M. Ward, Proliferative and nonproliferative lesions of the rat and mouse hepatobiliary system, *Toxicol. Pathol.* 38 (2010) 55–81S.
- [27] R.M. Tanguay, Y. Wu, E.W. Khandjian, Tissue-specific expression of heat shock proteins of the mouse in the absence of stress, *Dev. Genet.* 14 (1993) 112–118.
- [28] S. Marhenke, J. Lamle, L.E. Buitrago-Molina, J.M. Canon, R. Geffers, M. Finegold, M. Sporn, M. Yamamoto, M.P. Manns, M. Grompe, A. Vogel, Activation of nuclear factor E2-related factor 2 in hereditary tyrosinemia type 1 and its role in survival and tumor development, *Hepatology* 48 (2008) 487–496.
- [29] A. Vogel, I.E. van Den Berg, M. Al-Dhalimy, J. Groopman, C.N. Ou, O. Ryabinina, M.S. Iordanov, M. Finegold, M. Grompe, Chronic liver disease in murine hereditary tyrosinemia type 1 induces resistance to cell death, *Hepatology* 39 (2004) 433–443.
- [30] K. Manning, M. Al-Dhalimy, M. Finegold, M. Grompe, In vivo suppressor mutations correct a murine model of hereditary tyrosinemia type I, *Proc. Natl. Acad. Sci. U. S. A.* 96 (1999) 11928–11933.
- [31] L.E. Buitrago-Molina, S. Marhenke, T. Longerich, A.D. Sharma, A.E. Boukouris, R. Geffers, B. Guigas, M.P. Manns, A. Vogel, The degree of liver injury determines the role of p21 in liver regeneration and hepatocarcinogenesis in mice, *Hepatology* 58 (2013) 1143–1152.
- [32] E.A. Lock, P. Gaskin, M.K. Ellis, W. McLean Provan, M. Robinson, L.L. Smith, Tissue distribution of 2-(2-nitro-4-trifluoromethylbenzoyl)-cyclohexane-1,3-dione (NTBC) and its effect on enzymes involved in tyrosine catabolism in the mouse, *Toxicology* 144 (2000) 179–187.
- [33] M.C. Luijck, S.M. Jacobs, E.A. van Beurden, L.P. Koornneef, L.W. Klomp, R. Berger, I.E. van den Berg, Extensive changes in liver gene expression induced by hereditary tyrosinemia type I are not normalized by treatment with 2-(2-nitro-4-trifluoromethylbenzoyl)-1,3-cyclohexanedione (NTBC), *J. Hepatol.* 39 (2003) 901–909.
- [34] F.J. van Spronsen, C.M. Bijleveld, B.T. van Maldegem, F.A. Wijburg, Hepatocellular carcinoma in hereditary tyrosinemia type I despite 2-(2-nitro-4-3 trifluoromethylbenzoyl)-1, 3-cyclohexanedione treatment, *J. Pediatr. Gastroenterol. Nutr.* 40 (2005) 90–93.
- [35] B. Lindblad, S. Lindstedt, G. Steen, On the enzymic defects in hereditary tyrosinemia, *Proc. Natl. Acad. Sci. U. S. A.* 74 (1977) 4641–4645.
- [36] C. Laberge, A. Lescault, R.M. Tanguay, Hereditary tyrosinemias (type I): a new vista on tyrosine toxicity and cancer, *Adv. Exp. Med. Biol.* 206 (1986) 209–221.
- [37] R. Venugopal, A.K. Jaiswal, Nrf1 and Nrf2 positively and c-Fos and Fra1 negatively regulate the human antioxidant response element-mediated expression of NAD(P)H:quinone oxidoreductase1 gene, *Proc. Natl. Acad. Sci. U. S. A.* 93 (1996) 14960–14965.
- [38] K. Itoh, T. Chiba, S. Takahashi, T. Ishii, K. Igarashi, Y. Katoh, T. Oyake, N. Hayashi, K. Satoh, I. Hatayama, M. Yamamoto, Y. Nabeshima, An Nrf2/small Maf heterodimer mediates the induction of phase II detoxifying enzyme genes through antioxidant response elements, *Biochem. Biophys. Res. Commun.* 236 (1997) 313–322.
- [39] M. Zhu, W.E. Fahl, Functional characterization of transcription regulators that interact with the electrophile response element, *Biochem. Biophys. Res. Commun.* 289 (2001) 212–219.
- [40] M.K. Kwak, T.W. Kensler, R.A. Casero Jr., Induction of phase 2 enzymes by serum oxidized polyamines through activation of Nrf2: effect of the polyamine metabolite acrolein, *Biochem. Biophys. Res. Commun.* 305 (2003) 662–670.
- [41] J.M. Lee, P.C. Anderson, J.K. Padgett, J.M. Hanson, C.M. Waters, J.A. Johnson, Nrf2, not the estrogen receptor, mediates catechol estrogen-induced activation of the antioxidant responsive element, *Biochim. Biophys. Acta* 1629 (2003) 92–101.
- [42] X. Fang, S. Yu, A. Eder, M. Mao, R.C. Bast Jr., D. Boyd, G.B. Mills, Regulation of BAD phosphorylation at serine 112 by the Ras-mitogen-activated protein kinase pathway, *Oncogene* 18 (1999) 6635–6640.
- [43] L.W. Thomas, C. Lam, S.W. Edwards, Mcl-1; the molecular regulation of protein function, *FEBS Lett.* 584 (2010) 2981–2989.
- [44] E.M. Griner, M.G. Kazanietz, Protein kinase C and other diacylglycerol effectors in cancer, *Nat. Rev. Cancer* 7 (2007) 281–294.
- [45] C. Rosse, M. Linch, S. Kermorgant, A.J. Cameron, K. Boeckeler, P.J. Parker, PKC and the control of localized signal dynamics, *Nat. Rev. Mol. Cell Biol.* 11 (2010) 103–112.
- [46] L. Carduner, C.R. Picot, J. Leroy-Dudal, L. Blay, S. Kellouche, F. Carreiras, Cell cycle arrest or survival signaling through alphas integrins, activation of PKC and ERK1/2 lead to anoikis resistance of ovarian cancer spheroids, *Exp. Cell Res.* 320 (2014) 329–342.
- [47] S. Gillespie, X.D. Zhang, P. Hersey, Variable expression of protein kinase C epsilon in human melanoma cells regulates sensitivity to TRAIL-induced apoptosis, *Mol. Cancer Ther.* 4 (2005) 668–676.
- [48] M. Subramanian, C. Shaha, Up-regulation of Bcl-2 through ERK phosphorylation is associated with human macrophage survival in an estrogen microenvironment, *J. Immunol.* 179 (2007) 2330–2338.
- [49] G.L. Wong, H.L. Chan, Y.K. Tse, H.Y. Chan, C.H. Tse, A.O. Lo, V.W. Wong, On-treatment alpha-fetoprotein is a specific tumor marker for hepatocellular carcinoma in patients with chronic hepatitis B receiving entecavir, *Hepatology* 59 (2014) 986–995.
- [50] P. Russo, S. O'Regan, Visceral pathology of hereditary tyrosinemia type I, *Am. J. Hum. Genet.* 47 (1990) 317–324.
- [51] S. Lindstedt, E. Holme, E.A. Lock, O. Hjalmarson, B. Strandvik, Treatment of hereditary tyrosinemia type I by inhibition of 4-hydroxyphenylpyruvate dioxygenase, *Lancet* 340 (1992) 813–817.

- [52] M.K. Ellis, A.C. Whitfield, L.A. Gowans, T.R. Auton, W.M. Provan, E.A. Lock, L.L. Smith, Inhibition of 4-hydroxyphenylpyruvate dioxygenase by 2-(2-nitro-4-trifluoromethylbenzoyl)-cyclohexane-1,3-dione and 2-(2-chloro-4-methanesulfonylbenzoyl)-cyclohexane-1,3-dione, *Toxicol. Appl. Pharmacol.* 133 (1995) 12–19.
- [53] R.M. Tanguay, A. Bergeron, R. Jorquera, Hepatorenal tyrosinemia, in: R.P. Lifton, S. Somlo, D. Giebshi, D.W. Seldin (Eds.), *Genetic Diseases of the Kidney*, Elsevier, Place Published 2009, pp. 681–691.
- [54] S.B. Cullinan, D. Zhang, M. Hannink, E. Arvisais, R.J. Kaufman, J.A. Diehl, Nrf2 is a direct PERK substrate and effector of PERK-dependent cell survival, *Mol. Cell. Biol.* 23 (2003) 7198–7209.
- [55] W. Xu, C. Hellerbrand, U.A. Kohler, P. Bugnon, Y.W. Kan, S. Werner, T.A. Beyer, The Nrf2 transcription factor protects from toxin-induced liver injury and fibrosis, *Lab. Invest.* 88 (2008) 1068–1078.
- [56] Y. Tanaka, L.M. Aleksunes, R.L. Yeager, M.A. Gyamfi, N. Esterly, G.L. Guo, C.D. Klaassen, NF-E2-related factor 2 inhibits lipid accumulation and oxidative stress in mice fed a high-fat diet, *J. Pharmacol. Exp. Ther.* 325 (2008) 655–664.
- [57] S. Chowdhry, M.H. Nazmy, P.J. Meakin, A.T. Dinkova-Kostova, S.V. Walsh, T. Tsujita, J.F. Dillon, M.L. Ashford, J.D. Hayes, Loss of Nrf2 markedly exacerbates nonalcoholic steatohepatitis, *Free Radic. Biol. Med.* 48 (2010) 357–371.
- [58] L.R. Palam, T.D. Baird, R.C. Wek, Phosphorylation of eIF2 facilitates ribosomal bypass of an inhibitory upstream ORF to enhance CHOP translation, *J. Biol. Chem.* 286 (2011) 10939–10949.
- [59] R.N. Suragani, R.S. Zachariah, J.G. Velazquez, S. Liu, C.W. Sun, T.M. Townes, J.J. Chen, Heme-regulated eIF2 α kinase activated Atf4 signaling pathway in oxidative stress and erythropoiesis, *Blood* 119 (2012) 5276–5284.
- [60] K. Zhan, K.M. Vatter, B.N. Bauer, T.E. Dever, J.J. Chen, R.C. Wek, Phosphorylation of eukaryotic initiation factor 2 by heme-regulated inhibitor kinase-related protein kinases in *Schizosaccharomyces pombe* is important for resistance to environmental stresses, *Mol. Cell. Biol.* 22 (2002) 7134–7146.
- [61] N. Nemoto, T. Udagawa, T. Ohira, L. Jiang, K. Hirota, C.R. Wilkinson, J. Bahler, N. Jones, K. Ohta, R.C. Wek, K. Asano, The roles of stress-activated Sty1 and Gcn2 kinases and of the protooncogene homologue Int6/eIF3e in responses to endogenous oxidative stress during histidine starvation, *J. Mol. Biol.* 404 (2010) 183–201.
- [62] H.Y. Jiang, S.A. Wek, B.C. McGrath, D. Lu, T. Hai, H.P. Harding, X. Wang, D. Ron, D.R. Cavener, R.C. Wek, Activating transcription factor 3 is integral to the eukaryotic initiation factor 2 kinase stress response, *Mol. Cell. Biol.* 24 (2004) 1365–1377.
- [63] S.J. Marciniak, C.Y. Yun, S. Oyadomari, I. Novoa, Y. Zhang, R. Jungreis, K. Nagata, H.P. Harding, D. Ron, CHOP induces death by promoting protein synthesis and oxidation in the stressed endoplasmic reticulum, *Genes Dev.* 18 (2004) 3066–3077.
- [64] M.R. Chikka, D.D. McCabe, H.M. Tyra, D.T. Rutkowski, C/EBP homologous protein (CHOP) contributes to suppression of metabolic genes during endoplasmic reticulum stress in the liver, *J. Biol. Chem.* 288 (2013) 4405–4415.
- [65] D.T. Rutkowski, S.M. Arnold, C.N. Miller, J. Wu, J. Li, K.M. Gunnison, K. Mori, A.A. Sadighi Akha, D. Raden, R.J. Kaufman, Adaptation to ER stress is mediated by differential stabilities of pro-survival and pro-apoptotic mRNAs and proteins, *PLoS Biol.* 4 (2006), e374.
- [66] G.S. Hotamisligil, Endoplasmic reticulum stress and the inflammatory basis of metabolic disease, *Cell* 140 (2010) 900–917.
- [67] I. Tabas, D. Ron, Integrating the mechanisms of apoptosis induced by endoplasmic reticulum stress, *Nat. Cell Biol.* 13 (2011) 184–190.
- [68] C. Hetz, The unfolded protein response: controlling cell fate decisions under ER stress and beyond, *Nat. Rev. Mol. Cell Biol.* 13 (2012) 89–102.
- [69] A. Crozat, P. Aman, N. Mandahl, D. Ron, Fusion of CHOP to a novel RNA-binding protein in human myxoid liposarcoma, *Nature* 363 (1993) 640–644.
- [70] T.H. Rabbitts, A. Forster, R. Larson, P. Nathan, Fusion of the dominant negative transcription regulator CHOP with a novel gene FUS by translocation t(12;16) in malignant liposarcoma, *Nat. Genet.* 4 (1993) 175–180.
- [71] K. Oikawa, M. Tanaka, S. Itoh, M. Takanashi, T. Ozaki, Y. Muragaki, M. Kuroda, A novel oncogenic pathway by TLS-CHOP involving repression of MDA-7/IL-24 expression, *Br. J. Cancer* 106 (2012) 1976–1979.
- [72] D. DeZwaan-McCabe, J.D. Riordan, A.M. Arensdorf, M.S. Icardi, A.J. Dupuy, D.T. Rutkowski, The stress-regulated transcription factor CHOP promotes hepatic inflammatory gene expression, fibrosis, and oncogenesis, *PLoS Genet.* 9 (2013), e1003937.
- [73] A. Paine, B. Eiz-Vesper, R. Blasczyk, S. Immenschuh, Signaling to heme oxygenase-1 and its anti-inflammatory therapeutic potential, *Biochem. Pharmacol.* 80 (2010) 1895–1903.
- [74] H. Was, J. Dulak, A. Jozkowicz, Heme oxygenase-1 in tumor biology and therapy, *Curr. Drug Targets* 11 (2010) 1551–1570.
- [75] P. Banerjee, A. Basu, D. Datta, M. Gasser, A.M. Waaga-Gasser, S. Pal, The heme oxygenase-1 protein is overexpressed in human renal cancer cells following activation of the Ras-Raf-ERK pathway and mediates anti-apoptotic signal, *J. Biol. Chem.* 286 (2011) 33580–33590.
- [76] T. Yamamoto, N. Takano, K. Ishiwata, M. Ohmura, Y. Nagahata, T. Matsuura, A. Kamata, K. Sakamoto, T. Nakanishi, A. Kubo, T. Hishiki, M. Suematsu, Reduced methylation of PFKFB3 in cancer cells shunts glucose towards the pentose phosphate pathway, *Nat. Commun.* 5 (2014) 3480.
- [77] K. Nakamura, Y. Tanaka, H. Mitsubuchi, F. Endo, Animal models of tyrosinemia, *J. Nutr.* 137 (2007) 1556S–1560S (discussion 1573S–1575S).
- [78] G. Szabadkai, M.R. Duchen, Mitochondria: the hub of cellular Ca²⁺ signaling, *Physiology (Bethesda)* 23 (2008) 84–94.
- [79] P. Pinton, C. Giorgi, R. Síviero, E. Zecchini, R. Rizzuto, Calcium and apoptosis: ER-mitochondria Ca²⁺ transfer in the control of apoptosis, *Oncogene* 27 (2008) 6407–6418.
- [80] I. Kim, W. Xu, J.C. Reed, Cell death and endoplasmic reticulum stress: disease relevance and therapeutic opportunities, *Nat. Rev. Drug Discov.* 7 (2008) 1013–1030.
- [81] B. Bonneau, J. Prudent, N. Popgeorgiev, G. Gillet, Non-apoptotic roles of Bcl-2 family: the calcium connection, *Biochim. Biophys. Acta* 1833 (2013) 1755–1765.
- [82] J. Kang, M.G. Jeong, S. Oh, E.J. Jang, H.K. Kim, E.S. Hwang, A FoxO1-dependent, but NRF2-independent induction of heme oxygenase-1 during muscle atrophy, *FEBS Lett.* 588 (2014) 79–85.
- [83] M.S. Raab, I. Breitkreutz, G. Tonon, J. Zhang, P.J. Hayden, T. Nguyen, J.H. Fruehauf, B.K. Lin, D. Chauhan, T. Hideshima, N.C. Munshi, K.C. Anderson, K. Podar, Targeting PKC: a novel role for beta-catenin in ER stress and apoptotic signaling, *Blood* 113 (2009) 1513–1521.
- [84] J.A. McCubrey, L.S. Steelman, W.H. Chappell, S.L. Abrams, E.W. Wong, F. Chang, B. Lehmann, D.M. Terrian, M. Milella, A. Tafuri, F. Stivala, M. Libra, J. Basecke, C. Evangelisti, A.M. Martelli, R.A. Franklin, Roles of the Raf/MEK/ERK pathway in cell growth, malignant transformation and drug resistance, *Biochim. Biophys. Acta* 1773 (2007) 1263–1284.
- [85] F. Chang, L.S. Steelman, J.T. Lee, J.G. Shelton, P.M. Navolanic, W.L. Blalock, R.A. Franklin, J.A. McCubrey, Signal transduction mediated by the Ras/Raf/MEK/ERK pathway from cytokine receptors to transcription factors: potential targeting for therapeutic intervention, *Leukemia* 17 (2003) 1263–1293.
- [86] P.J. Roberts, C.J. Der, Targeting the Raf-MEK-ERK mitogen-activated protein kinase cascade for the treatment of cancer, *Oncogene* 26 (2007) 3291–3310.
- [87] D. Bregon, P.W. Doetsch, Transcriptional mutagenesis: causes and involvement in tumour development, *Nat. Rev. Cancer* 11 (2011) 218–227.